Published in final edited form as:
J Med Chem. 2013 September 12; 56(17): 6871–6885. doi:10.1021/jm400694d.

Exquisite Selectivity For Human Toll-like Receptor 8 in Substituted Furo[2,3-*c*]quinolines

Hari Prasad Kokatla[*], **Diptesh Sil**[*], **Subbalakshmi S. Malladi**[*], **Rajalakshmi Balakrishna**[*], **Alec R. Hermanson**[*], **Lauren M. Fox**[*], **Xinkun Wang**[†], **Anshuman Dixit**[‡], and **Sunil A. David**[*,§]

[*]Department of Medicinal Chemistry, University of Kansas, Lawrence, KS 66047, USA

[†]Genomics facility, University of Kansas, Lawrence, KS 66047, USA

[‡]Department of Translational Research and Technology Development, Institute of Life Sciences, Nalco Square, Bhubaneswar-751023, India

Abstract

Toll-like receptor (TLR)-8 agonists activate adaptive immune responses by inducing robust production of T helper 1-polarizing cytokines, suggesting that TLR8-active compounds may be promising candidate adjuvants. We synthesized and evaluated hitherto unexplored furo[2,3-*c*]quinolines and its regioisomeric furo[3,2-*c*]quinolines, derived via a tandem, one-pot Sonogashira coupling and intramolecular 5 *endo-dig* cyclization strategy, in a panel of primary screens. We observed a pure TLR8 agonistic activity profile in select furo[2,3-*c*]quinolines, with maximal potency conferred by a C2-butyl group (EC_{50}: 1.6 μM); shorter, longer, or substituted homologues, as well as compounds bearing C1 substitutions were inactive, which was rationalized by docking studies using the recently-described crystal structure of human TLR8. The best-in-class compound displayed prominent proinflammatory cytokine induction (including interleukin-12 and interleukin-18), but was bereft of interferon-α inducing properties, confirming its high selectivity for human TLR8.

Keywords

TLR8; TLR8 agonists; Vaccine adjuvants; Innate immunity; Furoquinolines; Sonogashira coupling

Introduction

Vaccines have played an indispensable role in the dramatic improvement in public health witnessed in modern times, particularly in the prevention of mortality and morbidity attributable to infectious diseases.[1] While the successes of active immunization beginning with Jenner's smallpox vaccine in 1796 are numerous and extraordinary, our failure to develop effective vaccines against diseases such as the human immunodeficiency virus (HIV), tuberculosis, and malaria have served to highlight deficiencies and shortcomings of the state-of-the-art in contemporary vaccine technology, catalyzing a renaissance in rational vaccine design and development.[2,3]

[§]*Corresponding Author Address:* Sunil A. David, Department of Medicinal Chemistry, University of Kansas, Multidisciplinary Research Building, Room 320D, 2030 Becker Drive, Lawrence KS 66047. Tel: 785-864-1610; Fax: 785-864-1961, sdavid@ku.edu.

Supporting Information Available: Characterization data (^{1}H, ^{13}C, mass spectra), LC-MS analyses of final compounds. This material is available free of charge via the Internet at http://pubs.acs.org.

A component that is being increasingly recognized as pivotal in the design of effective vaccines is the incorporation of appropriate immune potentiators (also termed adjuvants) along with the antigen. Adjuvants initiate early innate immune responses which subsequently lead to the induction of robust and long-lasting adaptive immune responses.[4] Aluminum salts (primarily phosphate and hydroxide), discovered by Glenny and coworkers,[5] have been the only adjuvants in clinical use until the recent approval of 3-*O*-desacyl-4'-monophosphoryl lipid A (MPL) by the FDA.[6] Aluminum salts are weak adjuvants for antibody induction, promoting a T helper 2 (Th2)-skewed, rather than a Th1 response;[7,8] they are virtually ineffective at inducing cytotoxic T lymphocyte or mucosal immunoglobulin A (IgA) antibody responses, and additionally, also appear to promote the induction of IgE isotype switching, which has been associated with allergic reactions in some subjects.[7,8]

Innate immune afferent signals activated by vaccine adjuvants include those originating from Toll-like receptors (TLRs), as well as retinoic acid-inducible gene 1 (RIG-I)-like receptors[9] and nucleotide oligomerization domain (NOD)-like receptors (NLRs).[10,11] There are 10 functional TLRs encoded in the human genome, which are trans-membrane proteins with an extracellular domain having leucine-rich repeats (LRR) and a cytosolic domain called the Toll/IL-1 receptor (TIR) domain.[12] The ligands for these receptors are highly conserved molecules such as lipopolysaccharides (LPS) (recognized by TLR4), lipopeptides (TLR2 in combination with TLR1 or TLR6), flagellin (TLR5), single stranded RNA (TLR7 and TLR8), double stranded RNA (TLR3), CpG motif-containing DNA (recognized by TLR9), and profilin present on uropathogenic bacteria (TLR11).[12] TLR1, −2, −4, −5, and −6 recognize extracellular stimuli, while TLR3, −7, −8 and −9 function within the endolysosomal compartment.[12] The activation of TLRs by their cognate ligands leads to production of inflammatory cytokines, and up-regulation of major histocompatibility complex (MHC) molecules and co-stimulatory signals in antigen-presenting cells (APCs) as well as activating natural killer (NK) cells (innate immune response), which leads to the priming and amplification of T-, and B-cell effector functions (adaptive immune responses).[13–16]

We have recently embarked on a systematic exploration[17,18] of a variety of TLR agonists with a view to identifying safe and potent vaccine adjuvants. The chemotypes that we have explored thus far include agonists of TLR2,[19–21] TLR7,[22–26] TLR8,[27,28] NOD1,[29] as well as C-C chemokine receptor type 1.[30]

Our efforts are currently focused on evaluating small molecule agonists of TLR8 as potential vaccine adjuvants. TLR8 is expressed in myeloid DCs, monocytes, and monocyte-derived dendritic cells, and engagement of TLR8 agonists induces a dominant proinflammatory cytokine profile including tumor necrosis factor-α (TNF-α), interleukin-12 (IL-12), and IL-18.[31] The prominent nuclear factor-κB (NF-κB)- and c-Jun *N*-terminal kinase-mediated stimulatory effects of TLR8-agonists on APCs [32,33] leads to robust Th1-type responses.[34] Unlike TLR2, −4, or −7 agonists, TLR8 agonists appear unique in markedly upregulating the production of Th1-polarizing cytokines TNF-α and IL-12 from neonatal APCs,[34] suggesting that TLR8 agonists may be useful as adjuvants for enhancing immune responses in newborns.

Furthermore, human T-regulatory cells (Tregs), classified immunophenotypically as naturally occurring ($CD4^+CD25^+Foxp3^+$) or induced ($CD4^+CD25^{high}$), down-regulate and suppress a broad array of immune responses, including the non-specific suppression of both $CD4^+$ and $CD8^+$ T-cells via cell-cell contact and via production of immunosuppressive cytokines such as IL-10 and transforming growth factor–β (TGF-β).[35–41] Tregs express abundant TLR8 mRNA, and TLR8 agonists have been shown to reverse Treg function via a

TLR8-MyD88 (myeloid differentiation factor 88)-IRAK4 (IL-1-receptor-associated kinase 4) signaling pathway.[42] Engagement and activation of TLR8 are, therefore, strongly associated with enhanced adaptive immune responses.

A prerequisite for the careful evaluation of TLR8 activators as potential adjuvants for neonatal vaccines is the availability of pure TLR8 agonists with negligible TLR7 activity and, other than the 2,3-diamino-furo[2,3-*c*]pyridine class of compounds recently described by us,[28] all other known agonists of TLR8 such as the imidazoquinolines (for instance, **1**),[25,43] thiazoloquinolines (CL075, **2**),[27,44–47] and a 2-aminobenzazepine derivative (VTX-2337, **3**),[48] all display mixed TLR7/TLR8-agonism, with the sole exception of VTX-294,[49] whose complete structure has not been reported. The structures of these mixed agonists are shown in Fig. 1. The 2,3-diamino-furo[2,3-*c*]pyridines are atypical and noncanonical in that although they activate TLR8-dependent NF-κB signaling, they are devoid of proinflammatory cytokine inducing activities.[28]

Driven by our desire to identify pure TLR8 agonists also capable of inducing IL-12 and IL-18, and drawing from our earlier work in delineating structure-activity relationships (SAR) in the furo[2,3-*c*]pyridines, we began exploring a variety of fused heterocyclic core structures. Our continuing investigations have led to the discovery of pure TLR8-agonistic activity associated with strong interferon-γ (IFN-γ), IL-12 and IL-18 inducing activities in a series of furo[2,3-*c*]quinolines. The 4-amino-furo[2,3-*c*]quinoline chemotype is unprecedented in the literature, and the activity profile of this class of compounds, examined by a range of secondary screens in human *ex vivo* blood models, including transcriptomal profiling, confirm pure TLR8 agonism with no detectable signatures of TLR7 activity, allowing for the first time a clear path toward the evaluation of such compounds as potential adjuvants for vaccines.

Results and Discussion

Our recent work on the 2,3-diamino-furo[2,3-*c*]pyridines, which displayed TLR8-dependent NF-κB signaling but dissociated from downstream cytokine induction led us to consider benzologues of the furo[2,3-*c*]pyridines. The 4-amino-furo[2,3-*c*]quinoline chemotype is hitherto not described in the literature, and presented a good starting point since its scaffold closely resembles known TLR7/8-active ligands. We envisioned that the furo[2,3-*c*]quinoline and its regioisomeric core structures could be derived via one-pot Sonogashira coupling of alkynes to either 4-iodoquinolin-3-ol (Scheme 1), or 3-iodoquinolin-4-ol (Scheme 2), followed by a tandem, tethered nucleophile-assisted, intramolecular 5 *endo-dig* cyclization.[50] Electrophilic iodination of commercially-available 3- and 4-hydroxyquinoline proceeded uneventfully using reported methods (Schemes 1 and 2, respectively).[51] One-pot Sonogashira coupling with a variety of alkynes, followed by 5-*endo-dig* cyclization yielded compounds the 2-substituted furo[2,3-*c*]quinolines **6a–y** (Scheme 1) and the regioisomeric furo[3,2-*c*]quinolines **11a–c** (Scheme 2) in good yields. The target compounds **8a–y** and **13a–c** bearing 4-amino groups were obtained using conventional procedures described previously.[23,27,44] Compounds **8a–y** and **13a–c** were screened in a panel of reporter gene assays for human TLR2/3/4/5/7/8/9 and NOD1/2 modulatory activities. We were fortunate that a distinct activity profile was observed in the very first set of compounds that were synthesized. Compounds **8b–f** showed pure TLR8 agonistic activity with maximal potency exhibited by **8d** with a C2-butyl group (EC_{50}: 1.6 μM, Fig. 2); shorter (**8b, 8c**) and longer (**8e, 8f**) homologues displayed lower agonistic potencies with the shortest analogue **8a** being inactive (Fig. 2). The dose-response profiles show characteristic biphasic responses (dose-dependent activation, followed by apparent suppression of NF-κB translocation, Fig. 2) as we had previously observed in several chemotypes.[23,28,52] We verified that the apparent

suppression was not due to cytotoxicity using LDH release and mitochondrial redox-based assays as described earlier by us.[53,54]

The SAR pattern with maximal activity conferred by a C2-butyl group is virtually identical to that found in TLR7-active imidazoquinolines,[23] and the TLR8/7-agonistic thiazoloquinolines,[27] but unlike the thiazoloquinolines,[27] **8d** was devoid of TLR7-stimulatory activities in primary screens (Fig. 2). The exquisite selectivity for TLR8 was confirmed in secondary screens using *ex vivo* whole human blood and PBMC models.[17] We had earlier shown that proinflammatory cytokine induction (TNF-α, IL-1β, IL-6 and IL-8) is a consequence of TLR8 activation.[18] Importantly, Th1-biasing IL-12 and IL-18 induction is also TLR8-dependent, while IFN-α production is TLR7-mediated.[24,52] We therefore examined cytokine and interferon induction profiles of **8d**, employing the thiazoloquinoline **2** as a reference compound. Unlike the 2,3-diamino-furo[2,3-*c*]pyridines,[28] **8d** was observed to induce TNF-α, IL-1β, IL-6 and IL-8 in a dose-dependent manner, albeit with a lower potency than **2** (Fig. 3). Compound **8d** induced IL-12 and IL-18, but was bereft of IFN-α-inducing properties (Fig. 4). The selectivity of **8d** for TLR8 was also reflected in the absence of natural killer lymphocyte activation[17,18] in human whole blood models as assessed by cluster of differentiation 69 (CD69) expression (Fig. 5), which we had previously shown to be TLR7-dependent.[17,18] Consistent with the above findings, transcriptomal profiling experiments showed strong induction of proinflammatory cytokine transcripts (including IL-12 and IL-18) by both **2** and **8d**, but IFN-α transcription was induced only by **2**, owing to its dual TLR8/7 agonistic activity (Table 1). These data collectively confirm the selectivity of **8d** for human TLR8.

Given that **8d** represents an optimized compound in a uniquely TLR8-specific chemotype, we also profiled cytokine- and chemokine-inducing properties using a 41-analyte, multiplexed assay, comparing **8d** to a variety of TLR agonists. We found that of the 41 analytes analyzed, whereas both **8d** and **2** induced granulocyte colony-stimulating factor (G-CSF), growth-related oncogene (GRO), and macrophage inflammatory proteins 1-α and -β (MIP-1α, MIP-1β), a highly potent, pure TLR7-agonistic imidazoquinoline (1-benzyl-2-butyl-1H–imidazo[4,5-c]quinolin-4-amine) that we had identified in our earlier SAR studies[23] did not (Fig. 6), indicating that this set of analytes could be useful in distinguishing TLR8-specific responses.

Distinct hints that the SAR in the 2-substituted furo[2,3-*c*]quinolines was much more stringent compared to the thiazoloquinolines[27] was evident right from the outset. C2 substituents with branched alkyl groups (**8g–i**) abrogated activity, and analogues with cycloaliphatic (**8j–8m**) or aromatic (**8n, 8o**) substituents were inactive, pointing to intolerance of steric bulk at the putative binding site(s). Since the crystal structure of TLR8 was not available at the time, we forged on, surmising that the introduction of polar H-bond donors (or acceptors) on the C2 alkyl group may help us better understand binding site interactions. We therefore examined a number of analogues bearing hydroxyl groups at various positions along the C2-alkyl chain (**8p–8v**), compounds with C2 substituents terminating with a primary amine (**8x, 8y**), as well as an analogue with an ether (H-bond acceptor) incorporated in the alkyl group (**8w**), but none of these compounds were active in any of our primary screens.

Mindful of our earlier observation that regioisomerism in the imidazoquinolines resulted in a switch from agonistic to antagonistic activities,[22,55] we also synthesized key regioisomeric furo[3,2-*c*]quinolines, **13a–c** (Scheme 2); these compounds were quiescent, displaying neither stimulatory nor inhibitory activity in primary screens. Given the fastidious structural requirements at the C2 position, we next synthesized a furo[2,3-*c*]isoquinoline with a C2-

butyl substituent (**18**, Scheme 3) in an order to explore chemical space beyond the fused-quinoline chemotypes, but were disappointed in that **18**, too, was inactive.

Reverting, therefore, to the C2-butyl furo[2,3-*c*]quinoline, we interrogated the effect of introducing substituents at the C1 position. We were, in particular, desirous of evaluating a C1-benzyl substituent, for this strategy had previously yielded highly potent, TLR7-selective agonists in the imidazoquinoline series.[23] Electrophilic bromination of **7d** furnished precursor **19** in good yield (Scheme 4) which was carried forward to obtain both the 1-bromo- and 1-benzyl-substituted analogues **21** and **24**, respectively (Scheme 4). Both analogues were found to be inactive.

As mentioned earlier, the 2,3-diamino-furo[2,3-*c*]pyridine class of compounds recently described by us[28] activate TLR8 but do not result in downstream cytokine production, suggesting an apparent dissociation between receptor occupancy, and signal transduction events leading to cytokine production, and it was of interest to compare SAR that we had gleaned from the furo[2,3-*c*]quinolines with select analogues of the 4-amino, C2-alkyl furo[2,3-*c*]pyridine series. Two such compounds (**28a, 28b**) were therefore synthesized (Scheme 5). Both these analogues retained TLR8-selective agonistic activities, but were substantially weaker (EC_{50}: 24.4 μM and 46.2 μM, respectively) than **8d** (EC_{50}: 1.6 μM).

Although at first glance our attempts at exploring SAR in the furo[2,3-*c*]quinolines had yielded a large number of inactive compounds, we are delighted in no small measure that we have finally arrived at pure TLR8 agonists that induce the expected complement of TLR8-mediated, Th1-biasing cytokine mediators, but are devoid of TLR7-dependent IFN-α-inducing properties. Just as we were concluding our studies on the furo[2,3-*c*]quinolines, crystal structures of hTLR8 complexed with mixed TLR7/TLR8-agonistic imidazoquinolines and thiazoloquinolines were reported,[56] allowing us to rationalize our experimentally-determined SAR on the pure TLR8-agonistic furo[2,3-*c*]quinolines. The crystal structure of human TLR8 in complex with **2** (PDB ID: 3W3K)[56] was used for docking studies. We employed induced-fit methods[57,58] in which the receptor sites were allowed conformational and torsional flexibility to simulate realistic ligand-receptor interactions to account for conformational changes in the binding site residues. **2** as well as **8d** occupy the same binding pocket formed by both the TLR8 protomers (Fig. 7A – B), with the binding geometry of these compounds and interacting residues being virtually identical (Fig. 7C – D). Strong ionic H-bonds (salt bridges) are observed between the C4-amine of both **2** and **8d** with Asp543 of protomer B, with additional stabilization derived from a H-bond between Thr574 (protomer B) and either the N^3 atom of the thiazole ring of **2**, or the oxygen atom of the furanyl ring of **8d**. π-π interactions of the quinoline moiety of **2** and **8d** (Phe405/Tyr353), as well as hydrophobic interactions of the C2-alkyl group (Phe346/Ile403/Gly376) occur exclusively with residues in protomer A (Fig. 7C – D). All of these interactions appear indispensable. The butyl group of **8d** allows for excellent nonpolar and van der Waals contacts in the rather shallow hydrophobic cavity, and homologues with increasing C2-chain length (**8e–8f**) dock poorly with kinked and sterically unfavorable conformations of the alkyl group. Analogues with cycloaliphatic (**8j–8m**) and aromatic substituents (**8n, 8o**) do not fit in the hydrophobic pocket at all, leading to unrealistic docked conformations (not shown). The cavity is lined entirely with side-chains of hydrophobic residues, explaining why even length-optimized analogues bearing polar groups at the C2 position such as **8r, 8u** and **8v** do not display TLR8 agonism. The feeble activity of the furopyridine compounds **28a** and **28b** imply significant contributions in binding free energies by π-π interactions of the quinoline moiety with Tyr353 and Phe405. The imposition of additional steric bulk at C1 (compound **24**) is not tolerated in the cleft bounded by Phe261 and Ser352 (Fig. 7D). Not only is pivotal ionic H-bond between the C4-amine of regioisomeric furo[3,2-*c*]quinoline **13b** and Asp543 weakened (3.8 Å), the

additional H-bond between the oxygen atom of the furan ring and Thr574 is lost, forcing **13b** to bind to TLR8 in an inverted fashion, with the C2-alkyl group facing the entrance to the binding site (Fig. 7E). Highly unfavorable H-bonds are also seen in the isoquinoline analogue **18**, especially with the loss of H-bonding of the furanyl oxygen (Fig. 7F).

In conclusion, an exploration of furo[2,3-*c*]quinolines have yielded pure TLR8 agonists, which are expected to possess strong Th1-biasing adjuvantic properties as evidenced by prominent IL-12 and IL-18 induction profiles, and are without IFN-α inducing properties, confirming its exquisite selectivity for human TLR8. The recently published atomic structure of human TLR8 has permitted a careful evaluation of SAR in this hitherto uncharacterized chemotype, and provides clear directions toward rational, structure-based ligand design. Immunization studies employing neonatal animal models are being planned with a view to comparing adjuvanticity of agonists with pure TLR7 and TLR8 agonistic properties vis-à-vis compounds with dual TLR7/8-stimulatory activities.

Experimental Section

Chemistry

All of the solvents and reagents used were obtained commercially and used as such unless noted otherwise. Moisture- or air-sensitive reactions were conducted under nitrogen atmosphere in oven-dried (120 °C) glass apparatus. The solvents were removed under reduced pressure using standard rotary evaporators. Flash column chromatography was carried out using RediSep Rf 'Gold' high performance silica columns on CombiFlash Rf instrument unless otherwise mentioned, while thin-layer chromatography was carried out on silica gel (200 μm) CCM pre-coated aluminum sheets. Purity for all final compounds was confirmed to be greater than 97% by LC-MS using a Zorbax Eclipse Plus 4.6 mm × 150 mm, 5 μm analytical reverse phase C18 column with H_2O-isopropanol or H_2O-CH_3CN gradients and an Agilent ESI-QTOF mass spectrometer (mass accuracy of 3 ppm) operating in the positive ion (or negative ion, as appropriate) acquisition mode.

Synthesis of 4-iodoquinolin-3-ol (5)

In an oven dried round bottom flask equipped with a stirring bar was placed 3-hydroxy quinoline (1.0 g, 6.89 mmol) in 2N NaOH (20 mL). To this mixture a solution of iodine (8.27 mmol) in 20% of aqueous potassium iodide (20 mL) was added drop-wise and stirred for 3 h at room temperature. The mixture was then acidified with acetic acid, and the precipitate was filtered and washed with water. After drying under vacuum, 1.50 g of **5** was obtained, which was used without purification. ^{1}H NMR (500 MHz, DMSO) δ 11.19 (s, 1H), 8.50 (s, 1H), 7.98 – 7.85 (m, 2H), 7.65 – 7.60 (m, 1H), 7.60 – 7.55 (m, 1H). ^{13}C NMR (126 MHz, DMSO) δ 152.2, 142.6, 141.3, 130.9, 129.9, 129.2, 128.5, 126.6, 94.5. MS (ESI) calculated for C_9H_6INO, m/z 270.95, found 271.96 $(M+H)^+$.

General procedure for Sonogashira reaction

To a stirred solution of 4-iodoquinolin-3-ol in acetonitrile:triethylamine (2:1) were added the appropriate alkyne (0.553 mmol), $Pd(PPh_3)_4$ (0.018 mmol) and CuI (0.018 mmol). The resulting reaction mixture was stirred at 70°C under nitrogen atmosphere for 12 h. After completion of reaction (monitored by TLC), the reaction mixture was diluted with water and extracted with ethylacetate (3 × 10 mL). The combined organic layer was dried over Na_2SO_4 and concentrated under reduced pressure, crude material was purified by flash chromatography using CH_2Cl_2:MeOH as an eluent.

2-propylfuro[2,3-*c*]quinoline (6c)

Yellow solid (60 mg, 78%). ^{1}H NMR (500 MHz, $CDCl_3$) δ 9.08 (s, 1H), 8.20 (d, *J* = 8.2 Hz, 1H), 8.07 (dd, *J* = 8.1, 1.2 Hz, 1H), 7.67 (ddd, *J* = 8.4, 6.9, 1.5 Hz, 1H), 7.60 (ddd, *J* = 8.1, 7.0, 1.2 Hz, 1H), 6.91 (d, *J* = 0.8 Hz, 1H), 2.91 – 2.86 (m, 2H), 1.91 – 1.82 (m, 2H), 1.06 (t, *J* = 7.4 Hz, 3H). ^{13}C NMR (126 MHz, $CDCl_3$) δ 163.0, 148.8, 144.3, 136.3, 131.4, 130.1, 127.3, 126.5, 123.7, 123.2, 101.1, 30.8, 21.2, 13.9. MS (ESI) calculated for $C_{14}H_{13}NO$, m/z 211.10, found 212.11 $(M+H)^+$.

2-butylfuro[2,3-*c*]quinoline (6d)

Yellow solid (70 mg, 83%). ^{1}H NMR (500 MHz, $CDCl_3$) δ 9.08 (d, *J* = 0.5 Hz, 1H), 8.19 (dd, *J* = 8.4, 0.5 Hz, 1H), 8.09 – 8.05 (m, 1H), 7.66 (ddd, *J* = 8.4, 6.9, 1.5 Hz, 1H), 7.60 (ddd, *J* = 8.1, 7.0, 1.2 Hz, 1H), 6.90 (d, *J* = 0.8 Hz, 1H), 2.92 (t, 2H), 1.82 (ddd, *J* = 15.2, 8.5, 6.7 Hz, 2H), 1.51 – 1.42 (m, 2H), 0.99 (t, *J* = 7.4 Hz, 3H). ^{13}C NMR (126 MHz, $CDCl_3$) δ 163.2, 148.8, 144.3, 136.4, 131.4, 130.1, 127.3, 126.5, 123.7, 123.2, 101.0, 29.9, 28.5, 22.4, 13.9. MS (ESI) calculated for $C_{15}H_{15}NO$, m/z : 225.11, found 226.13 $(M+H)^+$.

2-pentylfuro[2,3-*c*]quinoline (6e)

White solid (70 mg, 79%). ^{1}H NMR (500 MHz, $CDCl_3$) δ 9.08 (d, *J* = 0.7 Hz, 1H), 8.20 (dd, *J* = 8.4, 0.6 Hz, 1H), 8.07 (ddd, *J* = 8.1, 1.5, 0.6 Hz, 1H), 7.66 (ddd, *J* = 8.4, 6.9, 1.5 Hz, 1H), 7.60 (ddd, *J* = 8.1, 6.9, 1.3 Hz, 1H), 6.91 – 6.90 (m, 1H), 2.91 (t, *J* = 7.2 Hz, 2H), 1.88 – 1.80 (m, 2H), 1.46 – 1.35 (m, 4H), 0.93 (t, *J* = 7.1 Hz, 3H). ^{13}C NMR (126 MHz, $CDCl_3$) δ 163.3, 148.8, 144.3, 136.4, 131.4, 130.1, 127.4, 126.5, 123.7, 123.2, 101.0, 31.5, 28.8, 27.5, 22.5, 14.1. MS (ESI) calculated for $C_{16}H_{17}NO$, m/z : 239.13, found 240.14 $(M+H)^+$.

2-hexylfuro[2,3-*c*]quinoline (6f)

White solid (70 mg, 75%). ^{1}H NMR (500 MHz, $CDCl_3$) δ 9.08 (s, 1H), 8.20 (t, *J* = 8.3 Hz, 1H), 8.07 (dd, *J* = 8.1, 1.1 Hz, 1H), 7.66 (ddd, *J* = 8.4, 7.0, 1.5 Hz, 1H), 7.60 (ddd, 1H), 6.90 (d, *J* = 0.6 Hz, 1H), 2.91 (t, *J* = 7.6 Hz, 2H), 1.87 – 1.79 (m, 2H), 1.50 – 1.40 (m, 2H), 1.39 – 1.28 (m, 4H), 0.90 (t, *J* = 8.2, 5.9 Hz, 3H). ^{13}C NMR (126 MHz, $CDCl_3$) δ 163.2, 148.8, 144.3, 136.3, 131.4, 130.1, 127.3, 126.5, 123.7, 123.2, 101.0, 31.7, 29.0, 28.9, 27.8, 22.7, 14.2. MS (ESI) calculated for $C_{17}H_{19}NO$, m/z : 253.15, found 254.16 $(M+H)^+$.

2-isobutylfuro[2,3-*c*]quinoline (6g)

Liquid (120 mg, 72%). ^{1}H NMR (500 MHz, $CDCl_3$) δ 9.12 (s, 1H), 8.25 (d, *J* = 8.2 Hz, 1H), 8.08 (d, *J* = 7.9 Hz, 1H), 7.69 – 7.64 (m, 1H), 7.63 – 7.58 (m, 1H), 6.91 (s, 1H), 2.79 (dd, *J* = 7.1, 0.5 Hz, 2H), 2.20 (dp, *J* = 13.6, 6.8 Hz, 1H), 1.03 (d, *J* = 6.7 Hz, 6H). ^{13}C NMR (126 MHz, $CDCl_3$) δ 162.4, 144.3, 136.4, 131.5, 130.2, 127.4, 126.6, 123.7, 102.0, 38.0, 28.1, 22.6. MS (ESI) calculated for $C_{15}H_{15}NO$, m/z : 225.12, found 226.13 $(M+H)^+$.

2-(*tert*-butyl)furo[2,3-*c*]quinoline (6h)

White solid (69 mg, 83%). ^{1}H NMR (500 MHz, $CDCl_3$) δ 9.11 (s, 1H), 8.20 (d, *J* = 8.3 Hz, 1H), 8.08 (d, *J* = 7.9 Hz, 1H), 7.69 – 7.64 (m, 1H), 7.59 (t, *J* = 7.4 Hz, 1H), 6.89 (s, 1H), 1.47 (s, 9H). ^{13}C NMR (126 MHz, $CDCl_3$) δ 170.7, 148.8, 144.3, 136.4, 131.2, 130.1, 127.3, 126.5, 123.6, 123.4, 98.2, 33.6, 29.1. MS (ESI) calculated for $C_{15}H_{15}NO$, m/z : 225.12, found 226.14 $(M+H)^+$.

2-isopentylfuro[2,3-*c*]quinoline (6i)

Solid (65 mg, 74%). ^{1}H NMR (500 MHz, $CDCl_3$) δ 9.10 (s, 1H), 8.21 (d, *J* = 8.3 Hz, 1H), 8.07 (d, *J* = 7.9 Hz, 1H), 7.70 – 7.63 (m, 1H), 7.59 (t, 1H), 6.90 (s, 1H), 2.91 (t, 2H), 1.79 – 1.64 (m, 3H), 0.99 (d, *J* = 6.4 Hz, 6H). ^{13}C NMR (126 MHz, $CDCl_3$) δ 163.4, 148.8, 144.3,

136.3, 131.4, 130.2, 127.3, 126.5, 123.7, 123.2, 100.9, 36.7, 27.8, 26.8, 22.5. MS (ESI) calculated for $C_{16}H_{17}NO$, m/z : 239.13, found 240.14 $(M+H)^+$.

2-cyclopropylfuro[2,3-*c*]quinoline (6j)

Solid (60 mg, 78%). ^1H NMR (500 MHz, $CDCl_3$) δ 9.02 (d, *J* = 0.7 Hz, 1H), 8.17 (dd, *J* = 8.4, 0.6 Hz, 1H), 8.04 (ddd, *J* = 8.1, 1.5, 0.6 Hz, 1H), 7.66 (ddd, *J* = 8.4, 6.9, 1.5 Hz, 1H), 7.58 (ddd, *J* = 8.1, 6.9, 1.2 Hz, 1H), 6.89 – 6.85 (m, 1H), 2.21 – 2.14 (m, 1H), 1.12 (dqd, *J* = 6.0, 2.4, 1.2 Hz, 4H). ^{13}C NMR (126 MHz, $CDCl_3$) δ 164.0, 148.3, 144.4, 136.0, 131.7, 130.1, 127.4, 126.4, 123.7, 123.0, 99.4, 10.1, 8.5. MS (ESI) calculated for $C_{14}H_{11}NO$, m/z : 209.10, found 210.10 $(M+H)^+$.

2-cyclopentylfuro[2,3-*c*]quinoline (6k)

White solid (72 mg, 82%). ^1H NMR (500 MHz, $CDCl_3$) δ 9.08 (s, 1H), 8.20 (d, *J* = 8.3 Hz, 1H), 8.07 (d, *J* = 7.7 Hz, 1H), 7.70 – 7.64 (m, 1H), 7.59 (t, *J* = 11.0, 3.8 Hz, 1H), 6.91 (s, 1H), 3.41 – 3.31 (m, 1H), 2.23 – 2.13 (m, 2H), 1.95 – 1.81 (m, 4H), 1.81 – 1.69 (m, 2H). ^{13}C NMR (126 MHz, $CDCl_3$) δ 166.8, 144.3, 136.4, 131.3, 130.1, 127.3, 126.5, 123.7, 123.2, 99.6, 39.4, 32.1, 25.6. MS (ESI) calculated for $C_{16}H_{15}NO$, m/z : 237.11, found 238.13 $(M+H)^+$.

2-(cyclopentylmethyl)furo[2,3-*c*]quinoline (6l)

Solid (71 mg, 757%). ^1H NMR (500 MHz, $CDCl_3$) δ 9.10 (s, 1H), 8.22 (d, *J* = 8.2 Hz, 1H), 8.08 (d, *J* = 7.9 Hz, 1H), 7.67 (t, *J* = 7.0 Hz, 1H), 7.60 (t, 1H), 6.91 (s, 1H), 2.91 (d, *J* = 7.4 Hz, 2H), 2.38 (dt, *J* = 15.4, 7.8 Hz, 1H), 1.87 (m, 2H), 1.74 – 1.65 (m, 2H), 1.64 – 1.57 (m, 2H), 1.32 (m, 2H). ^{13}C NMR (126 MHz, $CDCl_3$) δ 163.0, 144.3, 136.4, 131.5, 130.2, 127.4, 126.5, 123.7, 101.5, 38.9, 34.9, 32.7, 25.2. MS (ESI) calculated for $C_{17}H_{17}NO$, m/z : 251.13, found 252.14 $(M+H)^+$.

2-(cyclohexylmethyl)furo[2,3-*c*]quinoline (6m)

Solid (170 mg, 87%). ^1H NMR (500 MHz, $CDCl_3$) δ 9.10 (s, 1H), 8.21 (d, *J* = 8.3 Hz, 1H), 8.07 (d, *J* = 7.7 Hz, 1H), 7.72 – 7.63 (m, 1H), 7.59 (t, *J* = 7.4 Hz, 1H), 6.89 (s, 1H), 2.78 (d, *J* = 6.9 Hz, 2H), 1.89 – 1.64 (m, 6H), 1.33 – 1.12 (m, 3H), 1.05 (qd, *J* = 12.4, 3.1 Hz, 2H). ^{13}C NMR (126 MHz, $CDCl_3$) δ 162.1, 148.8, 144.23, 136.4, 131.4, 130.1, 127.3, 126.5, 123.7, 123.2, 102.0, 37.3, 36.7, 33.3, 26.4, 26.2. MS (ESI) calculated for $C_{18}H_{19}NO$, m/z : 265.15, found 266.16 $(M+H)^+$.

2-phenylfuro[2,3-*c*]quinoline (6n)

White solid (65 mg, 72%). ^1H NMR (500 MHz, $CDCl_3$) δ 9.20 (d, 1H), 8.23 (dd, *J* = 8.3, 0.7 Hz, 1H), 8.17 (ddd, *J* = 8.0, 1.5, 0.5 Hz, 1H), 8.01 – 7.97 (m, 2H), 7.71 (ddd, *J* = 8.4, 6.9, 1.6 Hz, 1H), 7.65 (ddd, *J* = 8.1, 7.0, 1.3 Hz, 1H), 7.55 – 7.50 (m, 3H), 7.47 – 7.43 (m, 1H). ^{13}C NMR (126 MHz, $CDCl_3$) δ 158.8, 148.9, 144.5, 136.7, 131.6, 130.3, 129.8, 129.8, 129.2, 127.7, 126.9, 125.6, 123.7, 123.2, 99.9. MS (ESI) calculated for $C_{17}H_{11}NO$, m/z : 245.10, found 246.10 $(M+H)^+$.

furo[2,3-*c*]quinolin-2-ylmethanol (6p)

Solid (56 mg, 77%). ^1H NMR (500 MHz, MeOD) δ 9.07 (s, 1H), 8.26 (dd, *J* = 8.0, 1.2 Hz, 1H), 8.12 (d, *J* = 8.2 Hz, 1H), 7.77 – 7.71 (m, 1H), 7.71 – 7.66 (m, 1H), 7.39 (s, 1H), 4.84 (s, 2H). ^{13}C NMR (126 MHz, MeOD) δ 163.5, 150.2, 144.8, 137.2, 133.0, 129.7, 129.1, 128.3, 125.0, 124.6, 103.3, 58.1. MS (ESI) calculated for $C_{12}H_9NO_2$, m/z : 199.10, found 200.07 $(M+H)^+$.

2-(furo[2,3-*c*]quinolin-2-yl)ethanol (6q)

Solid (58 mg, 74%). ^{1}H NMR (500 MHz, MeOD) δ 9.02 (s, 1H), 8.23 (dd, 1H), 8.10 (dd, *J* = 8.3, 0.5 Hz, 1H), 7.71 (ddd, *J* = 8.5, 7.0, 1.6 Hz, 1H), 7.67 (ddd, *J* = 8.1, 7.0, 1.3 Hz, 1H), 7.26 (d, *J* = 0.7 Hz, 1H), 4.01 (t, *J* = 6.4 Hz, 2H), 3.17 (td, *J* = 6.4, 0.6 Hz, 2H). ^{13}C NMR (126 MHz, MeOD) δ 162.9, 149.9, 144.7, 136.7, 133.6, 129.6, 128.9, 128.0, 125.1, 124.4, 103.5, 60.6, 33.1. MS (ESI) calculated for $C_{13}H_{11}NO_2$, m/z : 213.08, found 214.09 $(M+H)^+$.

4-(furo[2,3-*c*]quinolin-2-yl)butan-1-ol (6s)

Solid (68 mg, 77%). ^{1}H NMR (500 MHz, MeOD) δ 8.99 (s, 1H), 8.22 – 8.18 (m, 1H), 8.09 (dd, *J* = 8.4, 0.6 Hz, 1H), 7.70 (ddd, *J* = 8.4, 6.9, 1.6 Hz, 1H), 7.65 (ddd, *J* = 8.1, 7.0, 1.3 Hz, 1H), 7.17 (d, *J* = 0.8 Hz, 1H), 3.63 (t, *J* = 6.4 Hz, 2H), 2.98 (t, 2H), 1.96 – 1.88 (m, 2H), 1.71 – 1.63 (m, 2H). ^{13}C NMR (126 MHz, MeOD) δ 165.5, 149.8, 144.7, 136.6, 133.6, 129.5, 128.9, 128.0, 125.1, 124.3, 102.4, 62.4, 33.0, 29.2, 25.2. MS (ESI) calculated for $C_{15}H_{15}NO_2$, m/z : 241.11, found 242.12 $(M+H)^+$.

2-(furo[2,3-*c*]quinolin-2-yl)propan-2-ol (6t)

White solid (60 mg, 72%). ^{1}H NMR (500 MHz, MeOD) δ 9.07 (d, *J* = 0.6 Hz, 1H), 8.29 – 8.24 (m, 1H), 8.14 – 8.10 (m, 1H), 7.73 (ddd, *J* = 8.5, 7.0, 1.6 Hz, 1H), 7.68 (ddd, *J* = 8.1, 7.0, 1.3 Hz, 1H), 7.36 (d, *J* = 0.8 Hz, 1H), 1.72 (s, 6H). ^{13}C NMR (126 MHz, MeOD) δ 169.7, 149.9, 144.8, 137.1, 133.0, 129.7, 129.0, 128.2, 125.0, 124.6, 100.6, 70.1, 29.1. MS (ESI) calculated for $C_{14}H_{13}NO_2$, m/z : 227.10, found 228.11 $(M+H)^+$.

1-(furo[2,3-*c*]quinolin-2-yl)propan-2-ol (6v)

White solid (70 mg, 84%). ^{1}H NMR (500 MHz, MeOD) δ 9.04 (d, *J* = 0.5 Hz, 1H), 8.27 – 8.23 (m, 1H), 8.11 (dd, *J* = 8.4, 0.6 Hz, 1H), 7.73 (ddd, *J* = 8.5, 7.0, 1.6 Hz, 1H), 7.68 (ddd, *J* = 8.1, 7.0, 1.3 Hz, 1H), 7.28 (d, *J* = 0.7 Hz, 1H), 4.32 – 4.25 (m, 1H), 3.09 (d, *J* = 6.2 Hz, 2H), 1.31 (d, *J* = 6.2 Hz, 3H). ^{13}C NMR (126 MHz, MeOD) δ 163.0, 149.9, 144.6, 136.7, 133.7, 129.5, 129.0, 128.1, 125.1, 124.4, 104.0, 67.1, 39.2, 23.4. MS (ESI) calculated for $C_{14}H_{13}NO_2$, m/z : 227.10, found 228.11 $(M+H)^+$.

2-(2-ethoxyethyl)furo[2,3-*c*]quinoline (6w)

Solid (70 mg, 77%). ^{1}H NMR (500 MHz, $CDCl_3$) δ 9.10 (s, 1H), 8.21 (d, *J* = 8.3 Hz, 1H), 8.08 (dd, *J* = 8.1, 1.1 Hz, 1H), 7.68 (ddd, *J* = 8.4, 7.0, 1.4 Hz, 1H), 7.63 – 7.59 (m, 1H), 7.02 (d, 1H), 3.87 (t, *J* = 6.6 Hz, 2H), 3.57 (q, *J* = 7.0 Hz, 2H), 3.20 (td, *J* = 6.6, 0.8 Hz, 2H), 1.23 (t, *J* = 7.0 Hz, 3H). ^{13}C NMR (126 MHz, $CDCl_3$) δ 160.1, 148.8, 144.3, 136.3, 131.4, 130.1, 127.3, 126.6, 123.7, 123.2, 102.3, 68.0, 66.7, 29.8, 15.3. MS (ESI) calculated for $C_{15}H_{15}NO_2$, m/z : 241.11, found 242.11 $(M+H)^+$.

2-(furo[2,3-*c*]quinolin-2-ylmethyl)isoindoline-1,3-dione (6x)

White solid (33 mg, 61%). ^{1}H NMR (500 MHz, DMSO) δ 9.20 (d, *J* = 0.5 Hz, 1H), 8.32 (d, 1H), 8.11 (dd, *J* = 8.3, 0.7 Hz, 1H), 7.96 (dd, *J* = 5.5, 3.0 Hz, 2H), 7.89 (dd, *J* = 5.5, 3.1 Hz, 2H), 7.75 – 7.64 (m, 3H), 5.11 (d, *J* = 0.4 Hz, 2H). ^{13}C NMR (126 MHz, DMSO) δ 167.3, 155.6, 148.3, 143.7, 136.6, 134.8, 131.6, 130.1, 129.6, 127.7, 126.9, 124.1, 123.5, 122.6, 103.8, 34.9. MS (ESI) calculated for $C_{20}H_{12}N_2O_3$, m/z : 328.08, found 329.10 $(M+H)^+$.

2-(2-(furo[2,3-*c*]quinolin-2-yl)ethyl)isoindoline-1,3-dione (6y)

White solid (65 mg, 77%). ^{1}H NMR (500 MHz, DMSO) δ 9.13 (s, 1H), 8.23 (dd, *J* = 8.0, 1.4 Hz, 1H), 8.10 (d, *J* = 8.2 Hz, 1H), 7.90 – 7.79 (m, 4H), 7.73 – 7.68 (m, 1H), 7.68 – 7.63 (m, 1H), 7.44 (s, 1H), 4.03 (t, *J* = 6.9 Hz, 2H), 3.30 (t, *J* = 6.9 Hz, 2H). ^{13}C NMR (126 MHz, DMSO) δ 167.7, 158.9, 148.5, 143.7, 136.2, 134.5, 131.6, 130.4, 129.5, 127.5, 126.7, 124.0,

123.2, 122.6, 103.1, 36.0, 27.3. MS (ESI) calculated for $C_{21}H_{14}N_2O_3$, m/z : 342.10, found 343.12 $(M+H)^+$.

General procedure for *N*-Oxidation

To a stirred solution of substrate (0.53 mmol) in $CHCl_3$ was added *m*-CPBA (1.06 mmol). The resulting reaction mixture was stirred at r.t. for 4 h. After completion of reaction (monitored by TLC), the reaction mixture was diluted with water and extracted with CH_2Cl_2 (3 × 10 mL). The combined organic layer was dried over Na_2SO_4, concentrated under reduced pressure, and the crude material was purified by flash chromatography.

2-methylfuro[2,3-*c*]quinoline 5-oxide (7b)

White solid (80 mg, 74%). ^1H NMR (500 MHz, $CDCl_3$) δ 8.86 (s, 1H), 8.84 (dd, 1H), 8.08 – 8.03 (m, 1H), 7.76 – 7.68 (m, 2H), 6.87 (t, 1H), 2.59 (d, *J* = 1.0 Hz, 3H). ^{13}C NMR (126 MHz, $CDCl_3$) δ 159.7, 147.2, 138.8, 129.0, 128.6, 124.5, 124.3, 122.7, 121.0, 102.2, 14.5. MS (ESI) calculated for $C_{12}H_9NO_2$, m/z : 199.10, found 200.06 $(M+H)^+$.

2-propylfuro[2,3-*c*]quinoline 5-oxide (7c)

White solid (78 mg, 72%). ^1H NMR (500 MHz, $CDCl_3$) δ 8.88 – 8.82 (m, 2H), 8.08 – 8.04 (m, 1H), 7.75 – 7.68 (m, 2H), 6.86 (dd, *J* = 1.7, 0.8 Hz, 1H), 2.88 – 2.83 (m, 2H), 1.88 – 1.79 (m, 2H), 1.05 (t, *J* = 7.4 Hz, 3H). ^{13}C NMR (126 MHz, $CDCl_3$) δ 163.7, 147.1, 138.8, 128.9, 128.5, 124.4, 124.2, 124.1, 122.8, 121.1, 101.4, 30.7, 21.1, 13.9. MS (ESI) calculated for $C_{14}H_{13}NO_2$, m/z : 227.10, found 228.10 $(M+H)^+$.

2-butylfuro[2,3-*c*]quinoline 5-oxide (7d)

White solid (75 mg, 70%). ^1H NMR (500 MHz, $CDCl_3$) δ 8.86 (d, *J* = 0.5 Hz, 1H), 8.85 – 8.83 (m, 1H), 8.08 – 8.04 (m, 1H), 7.75 – 7.68 (m, 2H), 6.86 (d, *J* = 0.9 Hz, 1H), 2.90 – 2.86 (m, 2H), 1.82 – 1.76 (m, 2H), 1.46 (dq, *J* = 14.7, 7.4 Hz, 2H), 0.98 (t, *J* = 7.4 Hz, 3H). ^{13}C NMR (126 MHz, $CDCl_3$) δ 164.0, 147.1, 138.7, 128.9, 128.5, 124.5, 124.2, 124.2, 122.8, 121.0, 101.3, 29.8, 28.5, 22.4, 13.9. MS (ESI) calculated for $C_{15}H_{15}NO_2$, m/z : 241.11, found 242.12 $(M+H)^+$.

2-pentylfuro[2,3-*c*]quinoline 5-oxide (7e)

White solid (77 mg, 72%). ^1H NMR (500 MHz, $CDCl_3$) δ 8.87 – 8.86 (m, 1H), 8.86 – 8.83 (m, 1H), 8.09 – 8.05 (m, 1H), 7.76 – 7.68 (m, 2H), 6.86 (d, *J* = 0.8 Hz, 1H), 2.87 (t, *J* = 7.4 Hz, 2H), 1.84 – 1.78 (m, 2H), 1.40 (qd, *J* = 4.6, 1.7 Hz, 2H), 0.93 (t, *J* = 7.1 Hz, 3H). ^{13}C NMR (126 MHz, $CDCl_3$) δ 164.0, 147.1, 138.7, 128.9, 128.5, 124.5, 124.2, 124.2, 122.8, 121.1, 101.3, 31.5, 28.8, 27.4, 22.5, 14.1. MS (ESI) calculated for $C_{16}H_{17}NO_2$, m/z : 255.12, found 256.14 $(M+H)^+$.

2-hexylfuro[2,3-*c*]quinoline 5-oxide (7f)

White solid (105 mg 82%). ^1H NMR (500 MHz, $CDCl_3$) δ 8.86 (d, *J* = 0.5 Hz, 1H), 8.86 – 8.82 (m, 1H), 8.08 – 8.05 (m, 1H), 7.75 – 7.68 (m, 2H), 6.86 (d, *J* = 0.9 Hz, 1H), 2.87 (t, *J* = 7.3 Hz, 2H), 1.80 (dt, *J* = 15.2, 7.5 Hz, 2H), 1.47 – 1.39 (m, 2H), 1.36 – 1.30 (m, 4H), 0.90 (t, *J* = 7.1 Hz, 3H). ^{13}C NMR (126 MHz, $CDCl_3$) δ 164.0, 147.1, 138.8, 128.9, 128.5, 124.5, 124.2, 124.2, 122.8, 121.1, 101.3, 31.6, 29.0, 28.8, 27.7, 22.7, 14.2. MS (ESI) calculated for $C_{17}H_{19}NO_2$, m/z : 269.14, found 270.15 $(M+H)^+$.

2-isobutylfuro[2,3-*c*]quinoline 5-oxide (7g)

Solid (100 mg, 78%). ^1H NMR (500 MHz, $CDCl_3$) δ 8.87 (s, 1H), 8.85 (dt, *J* = 7.2, 3.9 Hz, 1H), 8.09 – 8.06 (m, 1H), 7.76 – 7.69 (m, 2H), 6.88 (d, *J* = 0.7 Hz, 1H), 2.76 (dd, *J* = 7.1, 0.5

Hz, 2H), 2.22 – 2.12 (m, 1H), 1.03 (d, J = 6.7 Hz, 6H). ^{13}C NMR (126 MHz, $CDCl_3$) δ 163.0, 147.2, 138.8, 128.9, 128.5, 124.5, 124.3, 124.1, 122.8, 121.1, 102.3, 37.9, 28.0, 22.6. MS (ESI) calculated for $C_{15}H_{15}NO_2$, m/z : 241.11, found 242.13 $(M+H)^+$.

2-(*tert*-butyl)furo[2,3-*c*]quinoline 5-oxide (7h)

White solid (72 mg, 68%). ^{1}H NMR (500 MHz, $CDCl_3$) δ 8.88 (d, J = 0.6 Hz, 1H), 8.85 (dd, J = 7.8, 2.1 Hz, 1H), 8.09 – 8.06 (m, 1H), 7.75 – 7.69 (m, 2H), 6.85 (d, J = 0.9 Hz, 1H), 1.45 (s, 9H). ^{13}C NMR (126 MHz, $CDCl_3$) δ 171.5, 147.1, 138.7, 128.9, 128.5, 124.6, 124.2, 124.1, 123.0, 121.1, 98.6, 29.0. MS (ESI) calculated for $C_{15}H_{15}NO_2$, m/z : 241.11, found 242.12 $(M+H)^+$.

2-isopentylfuro[2,3-*c*]quinoline 5-oxide (7i)

Solid (60 mg, 77%). ^{1}H NMR (500 MHz, MeOD) δ 9.13 (d, J = 0.5 Hz, 1H), 8.72 (dd, J = 8.1, 1.6 Hz, 1H), 8.37 – 8.34 (m, 1H), 7.90 – 7.83 (m, 2H), 7.28 (d, J = 0.8 Hz, 1H), 3.01 – 2.96 (m, 2H), 1.78 – 1.72 (m, 2H), 1.72 – 1.65 (m, 1H), 1.01 (d, J = 6.5 Hz, 6H). ^{13}C NMR (126 MHz, MeOD) δ 167.7, 147.9, 138.8, 130.6, 130.5, 128.7, 126.7, 126.0, 124.0, 120.8, 102.8, 37.6, 28.9, 27.5, 22.7. MS (ESI) calculated for $C_{16}H_{17}NO_2$, m/z : 255.12, found 256.13 $(M+H)^+$.

2-cyclopropylfuro[2,3-*c*]quinoline 5-oxide (7j)

Solid (40 mg 74%). ^{1}H NMR (500 MHz, MeOD) δ 9.11 – 8.99 (m, 1H), 8.73 (t, J = 13.1 Hz, 1H), 8.36 – 8.30 (m, 1H), 7.96 – 7.78 (m, 2H), 7.24 (s, 1H), 2.35 – 2.24 (m, 1H), 1.27 – 1.16 (m, 2H), 1.15 – 1.09 (m, 2H). ^{13}C NMR (126 MHz, MeOD) δ 168.84, 130.7, 130.3, 129.8, 129.3, 126.0, 125.1, 123.6, 120.7, 100.9, 10.6, 9.2. MS (ESI) calculated for $C_{14}H_{11}NO_2$, m/z : 225.10, found 226.09 $(M+H)^+$.

2-cyclopentylfuro[2,3-*c*]quinoline 5-oxide (7k)

White solid (77 mg, 72%). ^{1}H NMR (500 MHz, MeOD) δ 9.12 (d, J = 0.4 Hz, 1H), 8.71 (dd, 1H), 8.35 (dd, 1H), 7.89 – 7.81 (m, 2H), 7.29 (d, J = 0.7 Hz, 1H), 3.47 – 3.39 (m, 1H), 2.26 – 2.14 (m, 2H), 1.96 – 1.85 (m, 4H), 1.81 – 1.72 (m, 2H). ^{13}C NMR (126 MHz, MeOD) δ 171.0, 147.9, 138.8, 130.6, 130.5, 128.7, 126.7, 126.0, 124.0, 120.8, 101.5, 40.5, 32.8, 26.4. MS (ESI) calculated for $C_{16}H_{15}NO_2$, m/z : 253.11, found 254.12 $(M+H)^+$.

2-(cyclopentylmethyl)furo[2,3-*c*]quinoline 5-oxide (7l)

White solid (75 mg, 70%). ^{1}H NMR (500 MHz, MeOD) δ 9.13 (s, 1H), 8.74 – 8.70 (m, 1H), 8.36 (dd, J = 7.5, 1.8 Hz, 1H), 7.91 – 7.82 (m, 2H), 7.29 (d, J = 0.5 Hz, 1H), 2.96 (d, J = 7.4 Hz, 2H), 2.44 – 2.37 (m, 1H), 1.93 – 1.85 (m, 2H), 1.75 – 1.67 (m, 2H), 1.65 – 1.58 (m, 2H), 1.40 – 1.32 (m, 2H). ^{13}C NMR (126 MHz, MeOD) δ 167.2, 147.9, 138.8, 130.6, 130.5, 128.7, 126.7, 126.0, 124.0, 120.8, 103.3, 40.0, 35.5, 33.5, 26.0. MS (ESI) calculated for $C_{17}H_{17}NO_2$, m/z : 267.12, found 268.14 $(M+H)^+$.

2-(cyclohexylmethyl)furo[2,3-*c*]quinoline 5-oxide (7m)

Solid (160 mg, 84%). ^{1}H NMR (500 MHz, $CDCl_3$) δ 8.87 (s, 1H), 8.84 (dd, 1H), 8.09 – 8.05 (m, 1H), 7.76 – 7.69 (m, 2H), 6.86 (d, J = 0.7 Hz, 1H), 2.76 (d, J = 6.8 Hz, 2H), 1.90 – 1.52 (m, 6H), 1.33 – 1.14 (m, 3H), 1.08 – 0.97 (m, 2H). ^{13}C NMR (126 MHz, $CDCl_3$) δ 162.9, 147.2, 138.7, 128.9, 128.5, 124.5, 124.3, 123.7, 122.8, 121.0, 102.3, 37.3, 36.6, 33.3, 29.9, 26.4, 26.2. MS (ESI) calculated for $C_{18}H_{19}NO_2$, m/z : 281.14, found 282.16 $(M+H)^+$.

2-phenylfuro[2,3-*c*]quinoline 5-oxide (7n)

White solid (73 mg, 68%). ^{1}H NMR (500 MHz, $CDCl_3$) δ 8.96 (d, *J* = 0.7 Hz, 1H), 8.89 – 8.85 (m, 1H), 8.17 (ddd, *J* = 3.2, 2.2, 0.5 Hz, 1H), 7.94 – 7.90 (m, 2H), 7.80 – 7.74 (m, 2H), 7.53 – 7.49 (m, 2H), 7.47 (d, *J* = 0.9 Hz, 1H), 7.46 – 7.42 (m, 1H). ^{13}C NMR (126 MHz, $CDCl_3$) δ 159.6, 147.5, 139.1, 129.9, 129.3, 129.3, 129.2, 128.8, 125.3, 124.5, 124.4, 124.3, 122.9, 121.2, 100.2. MS (ESI) calculated for $C_{17}H_{11}NO_2$, m/z : 261.08, found 262.09 $(M+H)^+$.

2-benzylfuro[2,3-*c*]quinoline 5-oxide (7o)

White solid (96 mg 90%). ^{1}H NMR (500 MHz, $CDCl_3$) δ 8.85 (d, *J* = 0.6 Hz, 1H), 8.83 (dd, 1H), 8.04 – 8.01 (m, 1H), 7.75 – 7.67 (m, 2H), 7.38 (ddd, *J* = 7.2, 4.4, 1.6 Hz, 2H), 7.35 – 7.30 (m, 3H), 6.82 (d, *J* = 0.9 Hz, 1H), 4.21 (s, 2H). ^{13}C NMR (126 MHz, $CDCl_3$) δ 162.0, 147.5, 138.9, 136.1, 129.1, 129.1, 129.0, 128.6, 127.4, 124.5, 124.2, 123.8, 122.8, 121.1, 102.7, 35.3. MS (ESI) calculated for $C_{18}H_{13}NO_2$, m/z : 275.10, found 276.11 $(M+H)^+$.

2-(hydroxymethyl)furo[2,3-*c*]quinoline 5-oxide(7p)

Yellow solid (77 mg, 79%).^{1}H NMR (500 MHz, MeOD) δ 9.15 (s, 1H), 8.72 (dd, *J* = 7.9, 1.8 Hz, 1H), 8.38 – 8.31 (m, 1H), 7.91 – 7.82 (m, 2H), 7.43 (d, *J* = 0.6 Hz, 1H), 4.82 (s, 2H). ^{13}C NMR (126 MHz, MeOD) δ 165.1, 148.4, 139.0, 130.7, 130.7, 127.8, 127.0, 125.9, 124.2, 120.9, 103.9, 57.9. MS (ESI) calculated for $C_{12}H_9NO_3$, m/z : 215.10, found 216.07 $(M+H)^+$.

2-(2-hydroxyethyl)furo[2,3-*c*]quinoline 5-oxide (7q)

White solid (75 mg, 78%)^{1}H NMR (500 MHz, MeOD) δ 9.09 (d, *J* = 0.5 Hz, 1H), 8.68 (dd, 1H), 8.31 – 8.27 (m, 1H), 7.88 – 7.78 (m, 2H), 7.29 (d, *J* = 0.8 Hz, 1H), 3.99 (t, *J* = 6.3 Hz, 2H), 3.15 (td, *J* = 6.3, 0.7 Hz, 2H). ^{13}C NMR (126 MHz, MeOD) δ 164.6, 147.9, 138.8, 130.6, 130.5, 128.5, 126.7, 125.9, 123.9, 120.8, 104.1, 60.5, 33.1. MS (ESI) calculated for $C_{13}H_{11}NO_3$, m/z : 229.10, found 230.09 $(M+H)^+$.

2-(3-hydroxypropyl)furo[2,3-*c*]quinoline 5-oxide (7r)

White solid (75 mg, 88%). ^{1}H NMR (500 MHz, MeOD) δ 9.13 (s, 1H), 8.75 – 8.69 (m, 1H), 8.38 – 8.33 (m, 1H), 7.90 – 7.82 (m, 2H), 7.30 (d, *J* = 0.9 Hz, 1H), 3.69 (t, *J* = 6.2 Hz, 2H), 3.06 (t, 2H), 2.10 – 2.00 (m, 2H). ^{13}C NMR (126 MHz, MeOD) δ 167.0, 148.0, 138.8, 130.6, 130.5, 128.7, 126.7, 126.0, 124.0, 120.8, 103.0, 61.8, 31.5, 26.0. MS (ESI) calculated for $C_{14}H_{13}NO_3$, m/z : 243.10, found 244.10 $(M+H)^+$.

2-(4-hydroxybutyl)furo[2,3-*c*]quinoline 5-oxide (7s)

Solid (60 mg, 76%). ^{1}H NMR (500 MHz, MeOD) δ 8.99 (s, 1H), 8.22 – 8.18 (m, 1H), 8.09 (dd, *J* = 8.4, 0.6 Hz, 1H), 7.70 (ddd, *J* = 8.4, 6.9, 1.6 Hz, 1H), 7.65 (ddd, *J* = 8.1, 7.0, 1.3 Hz, 1H), 7.17 (d, *J* = 0.8 Hz, 1H), 3.63 (t, *J* = 6.4 Hz, 2H), 2.98 (t, 2H), 1.96 – 1.88 (m, 2H), 1.71 – 1.63 (m, 2H). ^{13}C NMR (126 MHz, MeOD) δ 165.5, 149.8, 144.7, 136.6, 133.6, 129.5, 128.9, 128.0, 125.1, 124.3, 102.4, 62.4, 33.0, 29.2, 25.2. MS (ESI) calculated for $C_{15}H_{15}NO_3$, m/z : 257.10, found 258.11 $(M+H)^+$.

2-(2-hydroxypropan-2-yl)furo[2,3-*c*]quinoline 5-oxide (7t)

White solid (63 mg 74%). ^{1}H NMR (500 MHz, MeOD) δ 9.17 (s, 1H), 8.73 (d, 1H), 8.38 (dd, 1H), 7.92 – 7.83 (m, 2H), 7.42 (d, 1H), 1.70 (s, 6H). ^{13}C NMR (126 MHz, MeOD) δ 171.2, 148.0, 139.0, 130.8, 130.7, 127.9, 127.0, 126.0, 124.3, 120.9, 101.3, 70.0, 29.0. MS (ESI) calculated for $C_{14}H_{13}NO_3$, m/z : 243.10, found 244.10 $(M+H)^+$.

2-(1-hydroxy-3-methylbutyl)furo[2,3-*c*]quinoline 5-oxide (7u)

Solid (60 mg, 70%). ^{1}H NMR (500 MHz, MeOD) δ 9.18 (s, 1H), 8.74 (dd, 1H), 8.40 (dd, 1H), 7.92 – 7.85 (m, 2H), 7.46 (s, 1H), 4.98 (dd, *J* = 8.5, 5.1 Hz, 1H), 1.91 – 1.85 (m, 2H), 1.84 – 1.78 (m, 1H), 1.02 (dd, *J* = 6.3, 3.0 Hz, 6H). ^{13}C NMR (126 MHz, MeOD) δ 168.3, 148.1, 139.0, 130.7, 130.7, 127.9, 127.0, 126.0, 124.3, 120.9, 102.8, 66.9, 45.7, 25.7, 23.6, 22.3. MS (ESI) calculated for $C_{16}H_{17}NO_3$, m/z : 271.12, found 272.12 $(M+H)^+$.

2-(2-hydroxypropyl)furo[2,3-*c*]quinoline 5-oxide (7v)

Solid (65 mg, 81%). ^{1}H NMR (500 MHz, MeOD) δ 9.04 (d, *J* = 0.6 Hz, 1H), 8.63 – 8.60 (m, 1H), 8.27 – 8.24 (m, 1H), 7.80 – 7.72 (m, 2H), 7.23 (d, *J* = 0.7 Hz, 1H), 4.20 – 4.11 (m, 1H), 2.97 (ddd, *J* = 3.9, 2.6, 0.5 Hz, 2H), 1.21 (d, *J* = 6.2 Hz, 3H). ^{13}C NMR (126 MHz, MeOD) δ 164.5, 148.0, 138.8, 130.6, 130.5, 128.59, 126.8, 126.0, 124.0, 120.8, 104.6, 67.0, 39.2, 23.4. MS (ESI) calculated for $C_{14}H_{13}NO_3$, m/z : 243.10, found 244.10 $(M+H)^+$.

2-(2-ethoxyethyl)furo[2,3-*c*]quinoline 5-oxide (7w)

Solid (30 mg, 70%). ^{1}H NMR (500 MHz, MeOD) δ 9.15 (d, *J* = 0.7 Hz, 1H), 8.74 – 8.71 (m, 1H), 8.39 – 8.35 (m, 1H), 7.91 – 7.84 (m, 2H), 7.34 (d, *J* = 0.9 Hz, 1H), 3.89 (t, *J* = 6.3 Hz, 2H), 3.58 (q, *J* = 7.0 Hz, 2H), 3.24 – 3.21 (m, 2H), 1.19 (t, *J* = 7.0 Hz, 3H). ^{13}C NMR (126 MHz, MeOD) δ 164.7, 147.9, 138.9, 130.6, 130.6, 128.6, 126.8, 126.0, 124.0, 120.8, 103.9, 68.6, 67.4, 30.4, 15.4. MS (ESI) calculated for $C_{15}H_{15}NO_3$, m/z : 257.10, found 258.11 $(M+H)^+$.

2-((1,3-dioxoisoindolin-2-yl)methyl)furo[2,3-*c*]quinoline 5-oxide (7x)

Solid (33 mg, 61%). ^{1}H NMR (500 MHz, DMSO) δ 9.22 (s, 1H), 8.63 – 8.59 (m, 1H), 8.41 – 8.36 (m, 1H), 7.97 – 7.93 (m, 2H), 7.91 – 7.87 (m, 2H), 7.83 – 7.76 (m, 2H), 7.67 (d, *J* = 0.7 Hz, 1H), 5.06 (s, 2H). ^{13}C NMR (126 MHz, DMSO) δ 167.2, 155.4, 147.4, 138.5, 134.8, 131.6, 129.3, 128.6, 124.9, 124.1, 123.5, 122.4, 121.6, 120.0, 104.4, 34.7. MS (ESI) calculated for $C_{20}H_{12}N_2O_4$, m/z : 344.08, found 345.09 $(M+H)^+$.

2-(2-(1,3-dioxoisoindolin-2-yl)ethyl)furo[2,3-*c*]quinoline 5-oxide (7y)

Solid (65 mg, 77%). ^{1}H NMR (500 MHz, MeOD) δ 8.92 (d, *J* = 0.7 Hz, 1H), 8.70 (dd, *J* = 8.2, 1.5 Hz, 1H), 8.21 – 8.17 (m, 1H), 7.84 – 7.77 (m, 4H), 7.77 – 7.73 (m, 2H), 7.19 (d, *J* = 0.8 Hz, 1H), 4.15 (t, *J* = 6.7 Hz, 2H), 3.35 (t, *J* = 7.1, 6.5 Hz, 2H). ^{13}C NMR (126 MHz, MeOD) δ 168.9, 161.8, 147.5, 138.4, 135.0, 134.9, 132.4, 130.0, 130.0, 127.3, 125.8, 125.3, 124.0, 123.9, 123.4, 120.5, 104.0, 36.6, 28.3. MS (ESI) calculated for $C_{21}H_{14}N_2O_4$, m/z : 358.10, found 359.11 $(M+H)^+$.

General procedure for installation of the 4-amino group

To a stirred solution of *N*-oxide (0.414 mmol) in CH_2Cl_2 was added benzoylisocyanate (1.24 mmol). The resulting reaction mixture was stirred at 55°C for 2 h. After completion of reaction (monitored by TLC), the solvent was evaporated. The residue was re-dissolved in MeOH (4 mL), and NaOMe (2.07 mmole) was added and refluxed for 4 h. The solvent was evaporated and the crude material was purified by flash chromatography using CH_2Cl_2:MeOH as an eluent. For compounds **8x** and **8y**, after reaction with benzoylisocyanate (1st step), the solvent was evaporated, ethylenediamine (2 mL) was added and stirred at 70 °C for 12 h.

furo[2,3-*c*]quinolin-4-amine (8a)

Solid (16 mg, 68%). ^{1}H NMR (500 MHz, $CDCl_3$) δ 7.93 (ddd, *J* = 8.0, 1.5, 0.5 Hz, 1H), 7.81 (ddd, *J* = 8.4, 1.1, 0.5 Hz, 1H), 7.79 (d, *J* = 2.0 Hz, 1H), 7.55 (ddd, *J* = 8.5, 7.0, 1.5 Hz,

1H), 7.38 (ddd, *J* = 8.1, 7.0, 1.2 Hz, 1H), 7.20 (d, *J* = 2.0 Hz, 1H), 5.16 (s, 2H). ^{13}C NMR (126 MHz, $CDCl_3$) δ 146.4, 145.2, 144.3, 139.5, 129.9, 127.8, 126.6, 123.4, 123.1, 120.5, 106.2. HRMS (ESI) calculated for $C_{11}H_8N_2O$, m/z : 184.0637, found 185.0704 $(M+H)^+$.

2-methylfuro[2,3-*c*]quinolin-4-amine (8b)

Solid (35 mg, 70%). ^{1}H NMR (500 MHz, $CDCl_3$) δ 7.85 (ddd, *J* = 8.9, 5.0, 0.8 Hz, 2H), 7.55 (ddd, *J* = 8.4, 7.0, 1.5 Hz, 1H), 7.36 (ddd, *J* = 8.1, 7.1, 1.2 Hz, 1H), 6.81 (d, *J* = 1.0 Hz, 1H), 5.88 (s, 2H), 2.57 (d, *J* = 1.0 Hz, 3H). ^{13}C NMR (126 MHz, $CDCl_3$) δ 158.3, 144.9, 138.3, 132.0, 131.3, 129.7, 128.0, 125.3, 123.5, 123.1, 102.7, 14.5. HRMS (ESI) calculated for $C_{12}H_{10}N_2O$, m/z : 198.0793, found 199.0859 $(M+H)^+$.

2-propylfuro[2,3-*c*]quinolin-4-amine (8c)

Solid (38 mg, 78%). ^{1}H NMR (500 MHz, $CDCl_3$) δ 7.88 (dd, *J* = 8.0, 1.2 Hz, 1H), 7.81 – 7.76 (m, 1H), 7.52 (ddd, *J* = 8.4, 7.0, 1.5 Hz, 1H), 7.34 (ddd, *J* = 8.0, 7.0, 1.1 Hz, 1H), 6.81 (t, *J* = 0.8 Hz, 1H), 5.12 (s, 2H), 2.89 – 2.81 (m, 2H), 1.88 – 1.80 (m, 2H), 1.05 (t, *J* = 7.4 Hz, 3H). ^{13}C NMR (126 MHz, $CDCl_3$) δ 161.7, 144.8, 144.1, 138.6, 131.4, 127.6, 126.5, 123.4, 122.8, 120.4, 101.8, 30.7, 21.3, 13.9. HRMS (ESI) calculated for $C_{14}H_{14}N_2O$, m/z : 226.1106, found 227.1183 $(M+H)^+$.

2-butylfuro[2,3-*c*]quinolin-4-amine (8d)

Solid (39 mg, 80%). ^{1}H NMR (500 MHz, $CDCl_3$) δ 7.87 (ddd, *J* = 8.0, 1.4, 0.4 Hz, 1H), 7.80 – 7.76 (m, 1H), 7.52 (ddd, *J* = 8.4, 7.0, 1.5 Hz, 1H), 7.34 (ddd, *J* = 8.1, 7.0, 1.2 Hz, 1H), 6.80 (t, *J* = 0.8 Hz, 1H), 5.11 (s, 2H), 2.90 – 2.83 (m, 2H), 1.79 (ddd, *J* = 13.3, 8.5, 6.7 Hz, 2H), 1.51 – 1.40 (m, 2H), 0.98 (t, *J* = 7.4 Hz, 3H). ^{13}C NMR (126 MHz, $CDCl_3$) δ 161.9, 144.8, 144.1, 138.6, 131.3, 127.6, 126.5, 123.4, 122.8, 120.4, 101.7, 30.0, 28.4, 22.4, 13.9. HRMS (ESI) calculated for $C_{15}H_{16}N_2O$, m/z : 240.1263, found 241.1349 $(M+H)^+$.

2-pentylfuro[2,3-*c*]quinolin-4-amine (8e)

Solid (34 mg, 69%). ^{1}H NMR (500 MHz, $CDCl_3$) δ 7.88 (dd, *J* = 8.0, 1.1 Hz, 1H), 7.78 (dd, *J* = 8.4, 0.5 Hz, 1H), 7.52 (ddd, *J* = 8.4, 7.0, 1.5 Hz, 1H), 7.34 (ddd, *J* = 8.1, 7.0, 1.2 Hz, 1H), 6.80 (s, 1H), 5.09 (s, 2H), 2.88 – 2.83 (m, 2H), 1.84 – 1.77 (m, 2H), 1.46 – 1.34 (m, 4H), 0.93 (t, *J* = 7.1 Hz, 3H). ^{13}C NMR (126 MHz, $CDCl_3$) δ 161.9, 144.8, 144.2, 138.6, 131.3, 127.6, 126.5, 123.4, 122.8, 120.4, 101.7, 31.5, 28.7, 27.6, 22.5, 14.1. HRMS (ESI) calculated for $C_{16}H_{18}N_2O$, m/z : 254.1419, found 255.1496 $(M+H)^+$.

2-hexylfuro[2,3-*c*]quinolin-4-amine (8f)

Yellow solid (60 mg 67%). ^{1}H NMR (500 MHz, $CDCl_3$) δ 7.90 – 7.86 (m, 1H), 7.79 (dd, *J* = 8.4, 0.5 Hz, 1H), 7.52 (ddd, *J* = 8.5, 7.0, 1.5 Hz, 1H), 7.34 (ddd, *J* = 8.1, 7.0, 1.2 Hz, 1H), 6.80 (s, 1H), 5.21 (s, 2H), 2.86 (t, 2H), 1.84 – 1.76 (m, 2H), 1.47 – 1.39 (m, 2H), 1.38 – 1.29 (m, 4H), 0.91 (t, *J* = 7.1 Hz, 3H). ^{13}C NMR (126 MHz, $CDCl_3$) δ 161.8, 144.8, 138.4, 131.2, 128.6, 127.5, 126.2, 123.3, 122.7, 120.2, 101.5, 31.5, 28.9, 28.6, 27.8, 22.6, 14.1. HRMS (ESI) calculated for $C_{17}H_{20}N_2O$, m/z : 268.1576, found 269.1658 $(M+H)^+$.

2-isobutylfuro[2,3-*c*]quinolin-4-amine (8g)

Solid (55 mg, 70%). ^{1}H NMR (500 MHz, $CDCl_3$) δ 7.87 (ddd, *J* = 7.9, 1.4, 0.4 Hz, 1H), 7.80 (ddd, *J* = 8.5, 1.1, 0.5 Hz, 1H), 7.53 (ddd, *J* = 8.4, 7.0, 1.5 Hz, 1H), 7.34 (ddd, *J* = 8.1, 7.0, 1.2 Hz, 1H), 6.81 (s, 1H), 5.36 (s, 2H), 2.73 (dd, *J* = 7.1, 0.6 Hz, 2H), 2.15 (dp, *J* = 13.6, 6.8 Hz, 1H), 1.02 (d, *J* = 6.7 Hz, 6H). ^{13}C NMR (126 MHz, $CDCl_3$) δ 161.1, 144.9, 143.8, 138.6, 131.4, 127.6, 126.2, 123.4, 122.8, 120.2, 102.7, 37.9, 28.0, 22.6. HRMS (ESI) calculated for $C_{15}H_{16}N_2O$, m/z : 240.1263, found 241.1337 $(M+H)^+$.

2-(tert-butyl)furo[2,3-*c*]quinolin-4-amine (8h)

^{1}H NMR (500 MHz, $CDCl_3$) δ 7.89 (ddd, *J* = 8.0, 1.5, 0.5 Hz, 1H), 7.79 (dd, *J* = 8.4, 0.5 Hz, 1H), 7.53 (ddd, *J* = 8.4, 7.0, 1.5 Hz, 1H), 7.35 (ddd, *J* = 8.1, 7.0, 1.2 Hz, 1H), 6.80 (s, 1H), 5.27 (s, 2H), 1.45 (s, 9H). ^{13}C NMR (126 MHz, $CDCl_3$) δ 169.8, 144.8, 143.6, 138.4, 131.3, 127.7, 126.1, 123.4, 123.0, 120.4, 99.0, 33.6, 29.2. HRMS (ESI) calculated for $C_{15}H_{16}N_2O$, m/z : 240.1263, found 241.1342 $(M+H)^+$.

2-isopentylfuro[2,3-*c*]quinolin-4-amine (8i)

Solid (35 mg, 70%). ^{1}H NMR (500 MHz, $CDCl_3$) δ 7.87 (dd, *J* = 8.0, 1.0 Hz, 1H), 7.79 (dd, *J* = 8.4, 0.5 Hz, 1H), 7.53 (ddd, *J* = 8.4, 7.0, 1.5 Hz, 1H), 7.35 (ddd, *J* = 8.1, 7.1, 1.2 Hz, 1H), 6.81 (d, *J* = 0.8 Hz, 1H), 5.45 – 5.18 (m, 2H), 2.87 (t, 2H), 1.73 – 1.64 (m, 3H), 0.99 (d, *J* = 6.4 Hz, 6H). ^{13}C NMR (126 MHz, $CDCl_3$) δ 162.5, 144.8, 138.3, 131.6, 128.8, 127.8, 126.0, 123.4, 123.0, 120.2, 101.6, 36.8, 27.8, 26.7, 22.5. HRMS (ESI) calculated for $C_{16}H_{18}N_2O$, m/z : 254.1419, found 255.1496 $(M+H)^+$.

2-cyclopropylfuro[2,3-*c*]quinolin-4-amine (8j)

Solid (28 mg, 74%). ^{1}H NMR (500 MHz, $CDCl_3$) δ 7.85 (dd, *J* = 8.0, 1.1 Hz, 1H), 7.77 (dd, *J* = 8.4, 0.5 Hz, 1H), 7.52 (ddd, *J* = 8.4, 7.0, 1.5 Hz, 1H), 7.33 (ddd, *J* = 8.1, 7.0, 1.1 Hz, 1H), 6.78 – 6.75 (m, 1H), 5.15 – 5.03 (m, 2H), 2.14 (tt, *J* = 8.4, 5.1 Hz, 1H), 1.10 (tdd, *J* = 11.1, 7.0, 4.3 Hz, 2H), 1.05 – 0.99 (m, 2H). ^{13}C NMR (126 MHz, $CDCl_3$) δ 162.7, 144.5, 143.9, 137.9, 131.5, 127.5, 126.3, 123.3, 122.7, 120.1, 99.9, 29.7, 9.6, 8.0. HRMS (ESI) calculated for $C_{14}H_{12}N_2O$, m/z : 224.0950, found 225.1016 $(M+H)^+$.

2-cyclopentylfuro[2,3-*c*]quinolin-4-amine (8k)

Solid (40 mg, 68%). ^{1}H NMR (500 MHz, $CDCl_3$) δ 7.87 (dd, *J* = 8.0, 1.1 Hz, 1H), 7.78 (dd, *J* = 8.4, 0.5 Hz, 1H), 7.52 (ddd, *J* = 8.4, 7.0, 1.5 Hz, 1H), 7.34 (ddd, *J* = 8.1, 7.0, 1.2 Hz, 1H), 6.81 (d, *J* = 0.9 Hz, 1H), 5.13 (s, 2H), 3.35 – 3.27 (m, 1H), 2.20 – 2.11 (m, 2H), 1.89 – 1.82 (m, 3H), 1.79 – 1.70 (m, 3H). ^{13}C NMR (126 MHz, $CDCl_3$) δ 165.5, 144.8, 144.0, 138.5, 131.3, 127.6, 126.4, 123.4, 122.8, 120.4, 100.2, 39.3, 32.1, 29.9, 25.5. HRMS (ESI) calculated for $C_{16}H_{16}N_2O$, m/z : 252.1263, found 253.1338 $(M+H)^+$.

2-(cyclopentylmethyl)furo[2,3-*c*]quinolin-4-amine (8l)

Solid (44 mg, 75%). ^{1}H NMR (500 MHz, $CDCl_3$) δ 7.88 (ddd, *J* = 7.9, 1.4, 0.4 Hz, 1H), 7.78 (dd, *J* = 8.4, 0.6 Hz, 1H), 7.52 (ddd, *J* = 8.4, 7.0, 1.5 Hz, 1H), 7.34 (ddd, *J* = 8.1, 7.0, 1.2 Hz, 1H), 6.81 (s, 1H), 5.09 (s, 2H), 2.88 – 2.83 (m, 2H), 2.40 – 2.29 (m, 1H), 1.90 – 1.82 (m, 2H), 1.69 (qdd, *J* = 7.1, 6.7, 4.7 Hz, 2H), 1.64 – 1.54 (m, 2H), 1.36 – 1.26 (m, 2H). ^{13}C NMR (126 MHz, $CDCl_3$) δ 161.6, 144.8, 144.1, 138.6, 131.3, 127.6, 126.5, 123.4, 122.8, 120.4, 102.1, 38.9, 34.8, 32.7, 25.2. HRMS (ESI) calculated for $C_{17}H_{18}N_2O$, m/z : 266.1419, found 267.1495 $(M+H)^+$.

2-(cyclohexylmethyl)furo[2,3-*c*]quinolin-4-amine (8m)

White solid (75 mg, 71%). ^{1}H NMR (500 MHz, $CDCl_3$) δ 7.89 – 7.86 (m, 1H), 7.78 (dd, *J* = 8.4, 0.5 Hz, 1H), 7.52 (ddd, *J* = 8.4, 7.0, 1.5 Hz, 1H), 7.34 (ddd, *J* = 8.1, 7.1, 1.1 Hz, 1H), 6.79 (s, 1H), 5.19 (s, 2H), 2.74 (d, *J* = 6.6 Hz, 2H), 1.81 – 1.65 (m, 6H), 1.32 – 1.14 (m, 4H), 1.04 (qd, *J* = 12.9, 2.8 Hz, 1H). ^{13}C NMR (126 MHz, $CDCl_3$) δ 160.8, 144.9, 144.1, 138.6, 131.3, 127.6, 126.4, 123.4, 122.8, 120.4, 102.7, 37.4, 36.6, 33.3, 26.4, 26.3. HRMS (ESI) calculated for $C_{18}H_{20}N_2O$, m/z : 280.1576, found 281.1656 $(M+H)^+$.

2-phenylfuro[2,3-*c*]quinolin-4-amine (8n)

Solid (30 mg, 75%). ^{1}H NMR (500 MHz, $CDCl_3$) δ 7.97 (ddd, *J* = 8.0, 1.4, 0.4 Hz, 1H), 7.94 – 7.90 (m, 2H), 7.83 – 7.79 (m, 1H), 7.56 (ddd, *J* = 8.4, 7.0, 1.5 Hz, 1H), 7.53 – 7.48 (m, 2H), 7.45 – 7.41 (m, 2H), 7.39 (ddd, *J* = 8.1, 7.0, 1.2 Hz, 1H), 5.23 (s, 2H). ^{13}C NMR (126 MHz, $CDCl_3$) δ 157.8, 145.0, 144.4, 139.0, 131.7, 129.9, 129.5, 129.1, 127.9, 126.7, 125.3, 123.4, 123.1, 120.3, 100.8. HRMS (ESI) calculated for $C_{17}H_{12}N_2O$, m/z : 260.0950, found 261.1023 $(M+H)^+$.

2-benzylfuro[2,3-*c*]quinolin-4-amine (8o)

Solid (45 mg, 65%).^{1}H NMR (500 MHz, $CDCl_3$) δ 7.86 – 7.82 (m, 1H), 7.77 (dd, *J* = 8.4, 0.6 Hz, 1H), 7.52 (ddd, *J* = 8.4, 7.0, 1.5 Hz, 1H), 7.40 – 7.35 (m, 2H), 7.35 – 7.28 (m, 4H), 6.79 (t, *J* = 0.9 Hz, 1H), 5.10 (s, 2H), 4.21 (s, 2H). ^{13}C NMR (126 MHz, $CDCl_3$) δ 159.8, 144.9, 144.2, 139.0, 136.7, 131.2, 129.1, 129.0, 127.7, 127.2, 126.5, 123.4, 122.9, 120.4, 103.2, 35.2. HRMS (ESI) calculated for $C_{18}H_{14}N_2O$, m/z : 274.1106, found 275.1182 $(M+H)^+$.

(4-aminofuro[2,3-*c*]quinolin-2-yl)methanol (8p)

White solid (12 mg, 67%). ^{1}H NMR (500 MHz, DMSO) δ 8.00 (dd, *J* = 7.9, 1.2 Hz, 1H), 7.59 (d, *J* = 7.9 Hz, 1H), 7.45 (ddd, *J* = 8.4, 7.0, 1.5 Hz, 1H), 7.31 (s, 1H), 7.25 (ddd, *J* = 8.0, 7.0, 1.1 Hz, 1H), 6.78 (s, 2H), 4.67 (s, 2H). ^{13}C NMR (126 MHz, DMSO) δ 159.9, 146.1, 144.4, 138.6, 129.6, 127.1, 125.5, 123.5, 121.5, 119.4, 103.0, 56.4. HRMS (ESI) calculated for $C_{12}H_{10}N_2O_2$, m/z : 214.0742, found 215.0805 $(M+H)^+$.

2-(4-aminofuro[2,3-*c*]quinolin-2-yl)ethanol (8q)

White solid (20 mg, 65%). ^{1}H NMR (500 MHz, $CDCl_3$) δ 7.72 (d, *J* = 8.3 Hz, 1H), 7.65 (dd, *J* = 8.0, 1.1 Hz, 1H), 7.50 (ddd, *J* = 8.4, 5.9, 1.5 Hz, 1H), 7.30 – 7.26 (m, 1H), 6.79 (s, 1H), 5.28 (s, 2H), 4.10 (t, *J* = 6.0 Hz, 2H), 3.11 (t, *J* = 5.8 Hz, 2H). ^{13}C NMR (126 MHz, $CDCl_3$) δ 158.9, 144.6, 143.0, 138.3, 131.3, 127.8, 125.7, 123.4, 123.0, 119.8, 103.6, 60.5, 32.5. HRMS (ESI) calculated for $C_{13}H_{12}N_2O_2$, m/z : 228.0899, found 229.0962 $(M+H)^+$.

3-(4-aminofuro[2,3-*c*]quinolin-2-yl)propan-1-ol (8r)

Solid (70 mg, 75%). ^{1}H NMR (500 MHz, $CDCl_3$) δ 7.86 (dd, *J* = 8.0, 1.3 Hz, 1H), 7.78 (d, *J* = 8.3 Hz, 1H), 7.52 (ddd, *J* = 8.4, 7.1, 1.5 Hz, 1H), 7.37 – 7.32 (m, 1H), 6.84 (s, 1H), 5.24 (s, 2H), 3.78 (t, *J* = 6.2 Hz, 2H), 3.00 (t, *J* = 7.5 Hz, 2H), 2.12 – 2.03 (m, 2H). ^{13}C NMR (126 MHz, $CDCl_3$) δ 161.1, 144.8, 143.8, 138.6, 131.4, 127.8, 126.2, 123.4, 123.0, 120.2, 102.1, 61.8, 30.8, 25.1. HRMS (ESI) calculated for $C_{14}H_{14}N_2O_2$, m/z : 242.1055, found 243.1120 $(M+H)^+$.

4-(4-aminofuro[2,3-*c*]quinolin-2-yl)butan-1-ol (8s)

Solid (28 mg, 70%). ^{1}H NMR (500 MHz, MeOD) δ 7.95 – 7.91 (m, 1H), 7.65 (dd, *J* = 8.4, 0.5 Hz, 1H), 7.49 (ddd, *J* = 8.5, 7.0, 1.5 Hz, 1H), 7.31 (ddd, *J* = 8.1, 7.1, 1.1 Hz, 1H), 7.01 (s, 1H), 3.63 (t, *J* = 6.5 Hz, 2H), 2.94 (t, *J* = 7.5 Hz, 2H), 1.95 – 1.87 (m, 2H), 1.70 – 1.63 (m, 2H). ^{13}C NMR (126 MHz, MeOD) δ 163.9, 147.2, 144.2, 139.5, 133.0, 128.8, 125.5, 124.6, 123.7, 120.8, 102.8, 62.5, 33.0, 29.1, 25.3. HRMS (ESI) calculated for $C_{15}H_{16}N_2O_2$, m/z : 256.1212, found 257.1282 $(M+H)^+$.

2-(4-aminofuro[2,3-*c*]quinolin-2-yl)propan-2-ol (8t)

Solid (46 mg, 76%). ^{1}H NMR (500 MHz, $CDCl_3$) δ 7.77 – 7.71 (m, 2H), 7.52 – 7.47 (m, 1H), 7.29 (ddd, *J* = 8.1, 7.1, 1.0 Hz, 1H), 6.86 (s, 1H), 1.72 (s, 6H). ^{13}C NMR (126 MHz, $CDCl_3$) δ 165.5, 145.1, 143.3, 138.4, 130.8, 127.9, 125.8, 123.3, 123.1, 120.0, 100.3, 77.2,

69.2, 29.0. HRMS (ESI) calculated for $C_{14}H_{14}N_2O_2$, m/z : 242.1055, found 243.1123 (M +H)$^+$.

1-(4-aminofuro[2,3-*c*]quinolin-2-yl)-3-methylbutan-1-ol (8u)

Solid (35 mg, 77%). ^{1}H NMR (500 MHz, MeOD) δ 8.00 (d, 1H), 7.67 (d, *J* = 8.2 Hz, 1H), 7.53 (ddd, *J* = 8.4, 7.1, 1.4 Hz, 1H), 7.39 – 7.33 (m, 1H), 7.24 (d, *J* = 2.6 Hz, 1H), 4.96 (t, *J* = 6.7 Hz, 1H), 1.92 – 1.80 (m, 3H), 1.02 (dd, *J* = 6.2, 4.0 Hz, 6H). ^{13}C NMR (126 MHz, MeOD) δ 165.7, 147.3, 143.5, 132.8, 130.6, 129.2, 125.0, 124.7, 124.1, 120.6, 102.9, 66.9, 45.8, 25.7, 23.6, 22.3. HRMS MS (ESI) calculated for $C_{16}H_{18}N_2O_2$, m/z : 270.1368, found 271.1468 (M+H)$^+$.

1-(4-aminofuro[2,3-*c*]quinolin-2-yl)propan-2-ol (8v)

Solid (30 mg, 73%). ^{1}H NMR (500 MHz, MeOD) δ 7.96 (dd, *J* = 8.2, 1.3 Hz, 1H), 7.65 (dd, *J* = 8.4, 0.4 Hz, 1H), 7.50 (ddd, *J* = 8.5, 7.1, 1.5 Hz, 1H), 7.33 (ddd, *J* = 8.1, 7.1, 1.1 Hz, 1H), 7.10 (s, 1H), 4.29 – 4.22 (m, 1H), 3.05 – 3.01 (m, 2H), 1.30 (d, *J* = 6.2 Hz, 3H). ^{13}C NMR (126 MHz, MeOD) δ 161.3, 147.2, 144.0, 133.0, 130.4, 128.9, 125.3, 124.6, 123.8, 120.7, 104.4, 67.2, 39.0, 23.4. HRMS (ESI) calculated for $C_{14}H_{14}N_2O_2$, m/z : 242.1055, found 243.1121 (M+H)$^+$.

2-(2-ethoxyethyl)furo[2,3-*c*]quinolin-4-amine (8w)

Solid (15 mg, 71%). ^{1}H NMR (500 MHz, MeOD) δ 8.01 (ddd, *J* = 8.0, 2.3, 1.2 Hz, 1H), 7.68 (d, *J* = 8.2 Hz, 1H), 7.57 (t, *J* = 7.3 Hz, 1H), 7.45 – 7.38 (m, 1H), 7.16 (s, 1H), 3.89 (t, *J* = 6.4 Hz, 2H), 3.58 (q, *J* = 7.0 Hz, 2H), 3.20 (dt, *J* = 6.5, 3.1 Hz, 2H), 1.20 (t, *J* = 7.0 Hz, 3H). ^{13}C NMR (126 MHz, MeOD) δ 163.1, 146.51, 134.2, 133.1, 130.6, 129.7, 129.2, 125.0, 124.7, 123.3, 104.2, 68.9, 67.4, 30.3, 15.4. HRMS (ESI) calculated for $C_{15}H_{16}N_2O_2$, m/z : 256.1212, found 257.1280 (M+H)$^+$.

2-(aminomethyl)furo[2,3-*c*]quinolin-4-amine (8x)

Solid (24 mg, 65%). ^{1}H NMR (500 MHz, MeOD) δ 7.93 (dd, *J* = 8.0, 1.1 Hz, 1H), 7.65 (dd, *J* = 8.4, 0.4 Hz, 1H), 7.49 (ddd, *J* = 8.4, 7.0, 1.5 Hz, 1H), 7.31 (ddd, *J* = 8.1, 7.1, 1.1 Hz, 1H), 7.15 (s, 1H), 4.03 (s, 2H). ^{13}C NMR (126 MHz, MeOD) δ 162.7, 147.6, 145.0, 140.0, 132.4, 128.7, 126.0, 124.5, 123.6, 121.0, 102.9, 39.8. HRMS (ESI) calculated for $C_{12}H_{11}N_3O$, m/z : 213.0902, found 214.0967 (M+H)$^+$.

2-(2-aminoethyl)furo[2,3-*c*]quinolin-4-amine (8y)

Solid (25 mg, 66%). ^{1}H NMR (500 MHz, MeOD) δ 7.94 (dd, *J* = 8.0, 1.1 Hz, 1H), 7.64 (dd, *J* = 8.4, 0.5 Hz, 1H), 7.48 (ddd, *J* = 8.5, 7.0, 1.5 Hz, 1H), 7.30 (ddd, *J* = 8.1, 7.1, 1.1 Hz, 1H), 7.07 (s, 1H), 3.14 – 3.02 (m, 4H). ^{13}C NMR (126 MHz, MeOD) δ 161.1, 147.4, 145.0, 140.0, 132.6, 128.6, 126.0, 124.5, 123.5, 120.9, 103.7, 40.9, 32.7. HRMS (ESI) calculated for $C_{13}H_{13}N_3O$, m/z : 227.1059, found 228.1121 (M+H)$^+$.

Compound 10 was synthesized similarly as compound 5

3-iodoquinolin-4-ol (10)—Solid (1.6g). ^{1}H NMR (500 MHz, DMSO) δ 11.19 (s, 1H), 8.50 (s, 1H), 7.98 – 7.85 (m, 2H), 7.65 – 7.60 (m, 1H), 7.60 – 7.55 (m, 1H). ^{13}C NMR (126 MHz, DMSO) δ 152.2, 142.6, 141.3, 130.9, 129.9, 129.2, 128.5, 126.6, 94.5. MS (ESI) calculated for C_9H_6INO, m/z : 270.95, found 271.96 (M+H)$^+$.

Compounds 11a–11c were synthesized similarly as compound 6c

2-propylfuro[3,2-*c*]quinoline (11a)—Solid (55 mg, 71%). ^{1}H NMR (500 MHz, $CDCl_3$) δ 9.10 (s, 1H), 8.28 – 8.23 (m, 1H), 8.19 (dd, *J* = 8.0, 0.8 Hz, 1H), 7.67 (ddd, *J* = 8.5, 6.9, 1.6

Hz, 1H), 7.61 (ddd, *J* = 8.1, 7.0, 1.2 Hz, 1H), 6.60 (t, *J* = 0.9 Hz, 1H), 2.91 – 2.86 (m, 2H), 1.90 – 1.81 (m, 2H), 1.06 (t, *J* = 7.4 Hz, 3H). ^{13}C NMR (126 MHz, $CDCl_3$) δ 160.1, 155.1, 145.4, 145.2, 129.8, 127.8, 126.8, 121.6, 119.9, 117.3, 101.4, 30.5, 21.3, 13.9. MS (ESI) calculated for $C_{14}H_{13}NO$, m/z : 211.10, found 212.11 $(M+H)^+$.

2-butylfuro[3,2-*c*]quinoline (11b)—Solid (258 mg, 69%). ^{1}H NMR (500 MHz, $CDCl_3$) δ 9.13 (s, 1H), 8.25 (dd, *J* = 7.9, 1.6 Hz, 2H), 7.68 – 7.59 (m, 2H), 6.59 (t, *J* = 0.8 Hz, 1H), 2.94 – 2.87 (m, 2H), 1.81 (ddd, *J* = 15.2, 8.4, 6.7 Hz, 2H), 1.53 – 1.42 (m, 2H), 0.99 (t, *J* = 7.4 Hz, 3H). ^{13}C NMR (126 MHz, $CDCl_3$) δ 160.5, 155.1, 145.4, 145.3, 129.9, 127.9, 126.8, 121.7, 119.9, 117.3, 101.3, 30.0, 28.3, 22.4, 13.9. MS (ESI) calculated for $C_{15}H_{15}NO$, m/z : 225.11, found 226.13 $(M+H)^+$.

2-phenylfuro[3,2-*c*]quinoline (11c)—Solid (68 mg, 75%). ^{1}H NMR (500 MHz, $CDCl_3$) δ 9.18 (s, 1H), 8.38 (dd, *J* = 8.1, 1.2 Hz, 1H), 8.22 (d, *J* = 8.1 Hz, 1H), 7.98 – 7.93 (m, 2H), 7.74 – 7.64 (m, 2H), 7.51 (t, *J* = 7.7 Hz, 2H), 7.44 – 7.39 (m, 1H), 7.21 (s, 1H). ^{13}C NMR (126 MHz, $CDCl_3$) δ 156.6, 155.3, 145.9, 145.5, 130.0, 129.9, 129.1, 129.1, 128.3, 127.1, 125.1, 122.05, 120.1, 117.3, 100.6. MS (ESI) calculated for $C_{17}H_{11}NO$, m/z : 245.10, found 246.09 $(M+H)^+$.

Compounds 12a–12c were synthesized similarly as compound 7b

2-propylfuro[3,2-*c*]quinoline 5-oxide (12a)—Solid (88 mg, 82%). ^{1}H NMR (500 MHz, $CDCl_3$) δ 8.87 – 8.82 (m, 1H), 8.79 (s, 1H), 8.25 – 8.20 (m, 1H), 7.76 – 7.70 (m, 2H), 6.51 (t, *J* = 0.9 Hz, 1H), 2.89 – 2.83 (m, 2H), 1.89 – 1.80 (m, 2H), 1.06 (t, *J* = 7.4 Hz, 3H). ^{13}C NMR (126 MHz, $CDCl_3$) δ 162.2, 147.4, 138.7, 130.7, 129.1, 128.8, 121.3, 120.9, 120.6, 117.9, 101.2, 30.5, 21.2, 13.9. MS (ESI) calculated for $C_{14}H_{13}NO_2$, m/z : 227.10, found 228.10 $(M+H)^+$.

2-butylfuro[3,2-*c*]quinoline 5-oxide (12b)—Yellow solid (100 mg, 79%). ^{1}H NMR (500 MHz, $CDCl_3$) δ 8.88 – 8.82 (m, 1H), 8.79 (s, 1H), 8.26 – 8.20 (m, 1H), 7.76 – 7.70 (m, 2H), 6.51 (t, *J* = 0.9 Hz, 1H), 2.91 – 2.85 (m, 2H), 1.83 – 1.76 (m, 2H), 1.51 – 1.43 (m, 2H), 0.99 (t, *J* = 7.4 Hz, 3H). ^{13}C NMR (126 MHz, $CDCl_3$) δ 162.4, 147.4, 138.7, 130.7, 129.1, 128.8, 121.3, 121.0, 120.6, 117.9, 101.1, 29.9, 28.3, 22.4, 13.9. MS (ESI) calculated for $C_{15}H_{15}NO_2$, m/z : 241.11, found 242.12 $(M+H)^+$.

2-phenylfuro[3,2-*c*]quinoline 5-oxide (12c)—Solid (90 mg, 85%). ^{1}H NMR (500 MHz, $CDCl_3$) δ 8.90 – 8.86 (m, 2H), 8.37 – 8.33 (m, 1H), 7.94 – 7.90 (m, 2H), 7.78 (dd, *J* = 6.5, 3.3 Hz, 2H), 7.54 – 7.49 (m, 2H), 7.46 – 7.41 (m, 1H), 7.11 (s, 1H). ^{13}C NMR (126 MHz, $CDCl_3$) δ 158.4, 147.6, 139.3, 130.7, 129.7, 129.4, 129.2, 129.2, 125.2, 121.4, 121.4, 120.8, 118.1, 100.0. MS (ESI) calculated for $C_{17}H_{11}NO_2$, m/z : 261.10, found 262.09 $(M+H)^+$.

Compounds 13a–13c were synthesized similarly as compound 8a

2-propylfuro[3,2-*c*]quinolin-4-amine (13a)—Solid (35 mg, 71%). ^{1}H NMR (500 MHz, $CDCl_3$) δ 8.05 (dd, 1H), 7.76 (d, *J* = 8.2 Hz, 1H), 7.52 (ddd, *J* = 8.5, 7.0, 1.5 Hz, 1H), 7.34 (ddd, *J* = 8.1, 7.0, 1.1 Hz, 1H), 6.40 (t, *J* = 0.9 Hz, 1H), 5.10 (s, 2H), 2.86 – 2.81 (m, 2H), 1.87 – 1.78 (m, 2H), 1.04 (t, *J* = 7.4 Hz, 3H). ^{13}C NMR (126 MHz, $CDCl_3$) δ 159.1, 156.1, 151.9, 145.0, 128.2, 126.1, 122.9, 119.8, 114.7, 111.0, 99.7, 30.5, 21.4, 13.9. HRMS (ESI) calculated for $C_{14}H_{14}N_2O$, m/z : 226.1106, found 227.1177 $(M+H)^+$.

2-butylfuro[3,2-*c*]quinolin-4-amine (13b)—White solid (55 mg 69%). ^{1}H NMR (500 MHz, $CDCl_3$) δ 8.05 (ddd, *J* = 8.0, 1.5, 0.5 Hz, 1H), 7.79 – 7.73 (m, 1H), 7.52 (ddd, *J* = 8.5, 7.0, 1.5 Hz, 1H), 7.34 (ddd, *J* = 8.1, 7.0, 1.1 Hz, 1H), 6.39 (t, *J* = 0.9 Hz, 1H), 5.14 (s, 2H),

2.89 – 2.83 (m, 2H), 1.77 (ddd, *J* = 13.3, 8.5, 6.6 Hz, 2H), 1.50 – 1.41 (m, 2H), 0.98 (t, *J* = 7.4 Hz, 3H). ^{13}C NMR (126 MHz, $CDCl_3$) δ 159.3, 156.0, 151.9, 144.9, 128.3, 126.0, 123.0, 119.8, 114.7, 111.0, 99.6, 30.1, 28.2, 22.4, 13.9. HRMS (ESI) calculated for $C_{15}H_{16}N_2O$, m/z : 240.1263, found 241.1340 $(M+H)^+$.

2-phenylfuro[3,2-*c*]quinolin-4-amine (13c)—Solid (33 mg, 67%). ^{1}H NMR (500 MHz, MeOD) δ 8.93 (ddd, *J* = 8.0, 1.4, 0.4 Hz, 1H), 8.73 (dd, *J* = 8.4, 1.2 Hz, 2H), 8.47 – 8.44 (m, 1H), 8.35 – 8.31 (m, 1H), 8.31 – 8.27 (m, 2H), 8.21 – 8.12 (m, 3H). ^{13}C NMR (126 MHz, MeOD) δ 156.9, 156.5, 154.3, 145.9, 130.9, 129.7, 129.5, 129.4, 125.5, 125.6, 123.5, 120.6, 114.9, 112.9, 100.7, 49.0. HRMS (ESI) calculated for $C_{17}H_{12}N_2O$, m/z : 260.0950, found 261.1027 $(M+H)^+$.

Compound 15 was synthesized similarly as compound 5

4-iodoisoquinolin-3-ol (15)—Solid (1.4g). ^{1}H NMR (500 MHz, DMSO) δ 8.84 (s, 1H), 7.94 (d, *J* = 8.2 Hz, 1H), 7.76 (dd, *J* = 8.5, 0.6 Hz, 1H), 7.73 – 7.67 (m, 1H), 7.37 (ddd, *J* = 7.9, 6.8, 0.9 Hz, 1H). ^{13}C NMR (126 MHz, DMSO) δ 159.8, 149.4, 140.9, 132.8, 128.8, 128.5, 123.8, 123.5. MS (ESI) calculated for C_9H_6INO, m/z : 270.95, found 271.96 $(M+H)^+$.

Compound 16 was synthesized similarly as compound 6c

2-butylfuro[2,3-*c*]isoquinoline (16)—Solid (68 mg, 81%). ^{1}H NMR (500 MHz, $CDCl_3$) δ 8.87 (s, 1H), 8.06 (dd, *J* = 8.5, 0.8 Hz, 2H), 7.74 (ddd, *J* = 8.4, 6.9, 1.2 Hz, 1H), 7.57 – 7.52 (m, 1H), 6.85 (t, *J* = 0.9 Hz, 1H), 2.93 – 2.87 (m, 2H), 1.82 (ddd, *J* = 13.3, 8.5, 6.7 Hz, 2H), 1.46 (dq, *J* = 14.8, 7.4 Hz, 2H), 0.98 (t, *J* = 7.4 Hz, 3H). ^{13}C NMR (126 MHz, $CDCl_3$) δ 158.6, 158.3, 146.3, 131.3, 130.2, 128.8, 126.4, 125.2, 123.0, 114.4, 100.5, 29.9, 28.6, 22.4, 14.0. MS (ESI) calculated for $C_{15}H_{15}NO$, m/z : 225.12, found 226.12 $(M+H)^+$.

Compound 17 was synthesized similarly as compound 7b

2-butylfuro[2,3-*c*]isoquinoline 4-oxide (17)—Solid (20 mg, 74%). ^{1}H NMR (500 MHz, MeOD) δ 8.94 (s, 1H), 8.24 (dd, *J* = 8.3, 0.9 Hz, 1H), 8.08 (d, *J* = 8.4 Hz, 1H), 7.83 (ddd, *J* = 8.3, 7.0, 1.2 Hz, 1H), 7.70 (ddd, *J* = 8.2, 7.0, 1.1 Hz, 1H), 7.30 (t, *J* = 0.9 Hz, 1H), 3.03 – 2.97 (m, 2H), 1.90 – 1.83 (m, 2H), 1.54 – 1.46 (m, 2H), 1.02 (t, *J* = 7.4 Hz, 3H). ^{13}C NMR (126 MHz, MeOD) δ 162.3, 134.6, 134.6, 131.8, 131.1, 130.5, 128.9, 128.1, 124.2, 121.7, 103.5, 30.8, 28.9, 23.3, 14.1. MS (ESI) calculated for $C_{15}H_{15}NO_2$, m/z : 241.11, found 242.11 $(M+H)^+$.

Compound 18 was synthesized similarly as compound 8a

2-butylfuro[2,3-*c*]isoquinolin-5-amine (18)—Solid (15 mg, 62%). ^{1}H NMR (500 MHz, MeOD) δ 8.17 – 8.13 (m, 1H), 7.96 (ddd, *J* = 8.2, 1.1, 0.7 Hz, 1H), 7.69 (ddd, *J* = 8.2, 6.9, 1.1 Hz, 1H), 7.43 (ddd, *J* = 8.3, 6.9, 1.2 Hz, 1H), 6.74 (t, *J* = 0.9 Hz, 1H), 2.82 – 2.75 (m, 2H), 1.79 – 1.71 (m, 2H), 1.51 – 1.41 (m, 2H), 0.99 (t, *J* = 7.4 Hz, 3H). ^{13}C NMR (126 MHz, MeOD) δ 158.0, 156.0, 154.4, 134.4, 131.7, 125.9, 124.9, 124.1, 117.0, 106.1, 101.2, 31.3, 29.0, 23.3, 14.2. HRMS (ESI) calculated for $C_{15}H_{16}N_2O$, m/z : 240.1263, found 241.1350 $(M+H)^+$.

1-bromo-2-butylfuro[2,3-*c*]quinoline (19)—To a stirred solution of 2-butylfuro[2,3-c]quinoline **7d** (100 mg, 0.44 mmol) in CH_2Cl_2 was added bromine (80 μL, 1.55 mmol) and stirred at room temperature for 6 h. After completion of reaction (monitored by TLC), the solvent was evaporated, the crude material was purified by flash chromatography using CH_2Cl_2:MeOH to furnish **19** as yellow solid (50 mg, 75%). ^{1}H NMR (500 MHz, $CDCl_3$) δ 9.08 (s, 1H), 8.90 (d, *J* = 8.0 Hz, 1H), 8.22 (d, *J* = 8.3 Hz, 1H), 7.71 (ddd, *J* = 8.4, 7.0, 1.5 Hz, 1H), 7.68 – 7.63 (m, 1H), 2.98 – 2.92 (m, 2H), 1.84 – 1.76 (m, 2H), 1.44 (dq, *J* = 14.8,

7.4 Hz, 2H), 0.98 (t, *J* = 7.4 Hz, 3H). ^{13}C NMR (126 MHz, $CDCl_3$) δ 159.4, 147.4, 144.5, 136.2, 130.1, 127.9, 127.7, 126.8, 122.9, 122.3, 94.0, 29.6, 26.6, 22.4, 13.9. MS (ESI) calculated for $C_{15}H_{14}BrNO$, m/z : 303.03, found 304.04 $(M+H)^+$.

Compound 21 was synthesized similarly as compound 8a

1-bromo-2-butylfuro[2,3-*c*]quinolin-4-amine (21)—Solid (21 mg, 72%). ^{1}H NMR (500 MHz, MeOD) δ 8.67 (ddd, *J* = 8.2, 1.4, 0.5 Hz, 1H), 7.68 (ddd, *J* = 8.4, 1.1, 0.5 Hz, 1H), 7.53 (ddd, *J* = 8.5, 7.0, 1.5 Hz, 1H), 7.35 (ddd, *J* = 8.2, 7.0, 1.2 Hz, 1H), 2.97 (t, *J* = 7.5 Hz, 2H), 1.86 – 1.78 (m, 2H), 1.50 – 1.41 (m, 2H), 1.00 (t, *J* = 7.4 Hz, 3H). ^{13}C NMR (126 MHz, MeOD) δ 159.7, 147.2, 145.3, 138.9, 129.1, 128.5, 126.3, 123.4, 123.1, 120.4, 95.0, 30.7, 27.2, 23.3, 14.1. HRMS (ESI) calculated for $C_{15}H_{15}BrN_2O$, m/z : 318.0368, found 319.0429 $(M+H)^+$.

1-benzyl-2-butylfuro[2,3-*c*]quinoline (22)—To a stirred solution of **19** (50 mg, 0.164 mmol) in 1,4-dioxane were added 2-benzyl-4,4,5,5-tetramethyl-1,3,2-dioxaborolane (54 mg, 0.246 mmol), $Pd(dppf)Cl_2$ (8 mg, 0.009 mmol), Cs_2CO_3 (160 mg, 0.492 mmol) and 0.1 ml of water. The resulting reaction mixture was stirred at 70°C under nitrogen atmosphere for 12 h. After completion of reaction (monitored by TLC), the reaction mixture was diluted with water and extracted with ethylacetate (3 × 10 mL). The combined organic layer was dried over Na_2SO_4 and concentrated under reduced pressure, crude material was purified by flash chromatography using CH_2Cl_2:MeOH as an eluent to obtain **22** (24 mg, 92%). ^{1}H NMR (500 MHz, $CDCl_3$) δ 9.11 (d, *J* = 5.7 Hz, 1H), 8.19 – 8.14 (m, 1H), 7.94 (dd, *J* = 8.3, 0.8 Hz, 1H), 7.61 – 7.54 (m, 1H), 7.44 – 7.37 (m, 1H), 7.28 – 7.24 (m, 3H), 7.19 (dd, *J* = 10.3, 4.3 Hz, 2H), 4.38 (s, 2H), 2.91 – 2.86 (m, 2H), 1.80 – 1.72 (m, 2H), 1.44 – 1.35 (m, 2H), 0.93 (t, *J* = 7.4 Hz, 3H). ^{13}C NMR (126 MHz, $CDCl_3$) δ 159.8, 148.3, 144.7, 138.9, 136.5, 136.3, 130.3, 130.1, 128.9, 128.0, 127.4, 126.9, 126.6, 126.5, 123.6, 113.9, 101.0, 30.6, 30.5, 26.4, 22.6, 13.9. MS (ESI) calculated for $C_{22}H_{21}NO$, m/z : 315.20, found 316.18 $(M+H)^+$.

Compound 24 was synthesized similarly as compound 8a

1-benzyl-2-butylfuro[2,3-*c*]quinolin-4-amine (24)—Solid (31 mg, 75%). ^{1}H NMR (500 MHz, $CDCl_3$) δ 7.79 – 7.73 (m, 2H), 7.44 (ddd, *J* = 8.4, 7.0, 1.4 Hz, 1H), 7.30 – 7.23 (m, 3H), 7.23 – 7.18 (m, 2H), 7.15 (ddd, *J* = 8.2, 7.0, 1.2 Hz, 1H), 5.09 (s, 2H), 4.33 (s, 2H), 2.87 – 2.81 (m, 2H), 1.73 (ddd, *J* = 13.0, 8.5, 6.7 Hz, 2H), 1.39 (dq, *J* = 14.7, 7.4 Hz, 2H), 0.92 (t, *J* = 7.4 Hz, 3H). ^{13}C NMR (126 MHz, CDCl3) δ 158.4, 144.9, 144.4, 139.1, 138.2, 130.0, 128.8, 128.0 (2C), 127.2 (2C), 126.6, 126.6, 123.4, 122.8, 121.0, 114.7, 30.7, 30.4, 26.3, 22.6, 13.9. HRMS (ESI) calculated for $C_{22}H_{22}N_2O$, m/z : 330.1732, found 331.1808 $(M+H)^+$.

Compounds 27a–b were synthesized similarly as compound 7b

2-propylfuro[2,3-*c*]pyridine 6-oxide (27a)—Oil (85 mg, 78%). ^{1}H NMR (500 MHz, $CDCl_3$) δ 8.48 (s, 1H), 8.08 (dd, *J* = 6.7, 1.5 Hz, 1H), 7.30 (d, *J* = 6.7 Hz, 1H), 6.41 (d, *J* = 0.8 Hz, 1H), 2.75 (t, *J* = 7.5 Hz, 2H), 1.81 – 1.72 (m, 2H), 1.00 (t, *J* = 7.4 Hz, 3H). ^{13}C NMR (126 MHz, $CDCl_3$) δ 165.3, 152.0, 135.0, 128.5, 124.7, 115.8, 102.0, 30.5, 20.8, 13.8. MS (ESI) calculated for $C_{10}H_{11}NO_2$, m/z : 177.08, found 178.08 $(M+H)^+$.

2-butylfuro[2,3-*c*]pyridine 6-oxide (27b)—Oil (80 mg, 73%). ^{1}H NMR (500 MHz, $CDCl_3$) δ 8.52 – 8.47 (m, 1H), 8.10 (dd, *J* = 6.7, 1.5 Hz, 1H), 7.31 (d, *J* = 6.7 Hz, 1H), 6.42 (d, *J* = 0.9 Hz, 1H), 2.79 (t, 2H), 1.78 – 1.67 (m, 2H), 1.48 – 1.37 (m, 2H), 0.96 (t, *J* = 7.4 Hz, 3H). ^{13}C NMR (126 MHz, $CDCl_3$) δ 165.5, 152.0, 135.1, 128.4, 124.8, 115.8, 101.9,

29.5, 28.3, 22.4, 13.9. MS (ESI) calculated for $C_{11}H_{13}NO_2$, m/z : 191.09, found 192.10 (M +H)$^+$.

Compounds 28a–b was synthesized similarly as compound 8a

2-propylfuro[2,3-*c*]pyridin-7-amine (28a)—Oil (33 mg, 67%). ^{1}H NMR (500 MHz, $CDCl_3$) δ 7.80 (d, *J* = 5.5 Hz, 1H), 6.85 (d, *J* = 5.5 Hz, 1H), 6.34 (t, *J* = 0.8 Hz, 1H), 4.67 (s, 2H), 2.79 – 2.71 (m, 2H), 1.82 – 1.74 (m, 2H), 1.01 (t, *J* = 7.4 Hz, 3H). ^{13}C NMR (126 MHz, $CDCl_3$) δ 161.8, 144.1, 140.5, 139.2, 135.3, 107.5, 102.4, 30.6, 21.1, 13.9. HRMS (ESI) calculated for $C_{10}H_{12}N_2O$, m/z : 176.0950, found 177.1067 (M+H)$^+$.

2-butylfuro[2,3-*c*]pyridin-7-amine (28b)—Oil (35 mg, 71%). ^{1}H NMR (500 MHz, $CDCl_3$) δ 7.80 (d, *J* = 5.5 Hz, 1H), 6.85 (d, *J* = 5.5 Hz, 1H), 6.33 (t, *J* = 0.8 Hz, 1H), 4.68 (s, 2H), 2.80 – 2.74 (m, 2H), 1.77 – 1.69 (m, 2H), 1.47 – 1.38 (m, 2H), 0.96 (t, *J* = 7.4 Hz, 3H). ^{13}C NMR (126 MHz, $CDCl_3$) δ 162.0, 144.0, 140.4, 139.2, 135.3, 107.5, 102.3, 29.8, 28.3, 22.4, 13.9. HRMS (ESI) calculated for $C_{11}H_{14}N_2O$, m/z: 190.1106, found 191.1231 (M+H)$^+$.

Human TLR2/–3/–4/–5/–7/–8/–9 Reporter Gene assays (NF-κB induction)

The induction of NF-κB was quantified using human TLR2/–3/–4/–5/–7/–8/–9-specific HEK-Blue™ reporter gene assays as previously described by us.[17,22,23] HEK293 cells stably co-transfected with the appropriate hTLR, MD2, and secreted alkaline phosphatase (sAP), were maintained in HEK-Blue™ Selection medium containing zeocin and normocin. Stable expression of secreted alkaline phosphatase (sAP) under control of NF-κB/AP-1 promoters is inducible by appropriate TLR agonists, and extracellular sAP in the supernatant is proportional to NF-κB induction. HEK-Blue™ cells were incubated at a density of ~10^5 cells/ml in a volume of 80 μl/well, in 384-well, flat-bottomed, cell culture-treated microtiter plates until confluency was achieved, and subsequently stimulated with graded concentrations of stimuli. sAP was assayed spectrophotometrically using an alkaline phosphatase-specific chromogen (present in HEK-detection medium as supplied by the vendor) at 620 nm.

Immunoassays for cytokines

Fresh human peripheral blood mononuclear cells (hPBMC) were isolated from human blood obtained by venipuncture with informed consent and as per institutional guidelines on Ficoll-Hypaque gradients as described elsewhere.[59] Aliquots of PBMCs (10^5 cells in 100 μL/well) were stimulated for 12 h with graded concentrations of test compounds. Supernatants were isolated by centrifugation, and were assayed in triplicates using analyte-specific multiplexed cytokine/chemokine bead array assays as reported by us previously.[60] PBMC supernatants were also analyzed for 41 chemokines and cytokines (EGF, Eotaxin, FGF-2, Flt-3 ligand, Fractalkine, G-CSF, GM-CSF, GRO, IFN-α2, IFN-γ, IL-10, IL-12 (p40), IL-12 (p70), IL-13, IL-15, IL-17, IL-1ra, IL-1α, IL-1β, IL-2, IL-3, IL-4, IL-5, IL-6, IL-7, IL-8, IL-9, IP-10, MCP-1, MCP-3, MDC (CCL22), MIP-1α, MIP-1β, PDGF-AA, PDGF-AB/BB, RANTES, TGFα, TNF-α, TNF-β, VEGF, sCD40L) using a magnetic bead-based multiplexed assay kit (Milliplex MAP Human Cytokine/Chemokine kit). Data were acquired and processed on a MAGPIX instrument (EMD Millipore, Billerica, MA) with an intra-assay coefficients of variation ranging from 4–8% for the 41 analytes.

Flow-cytometric immunostimulation experiments

CD69 upregulation was determined by flow cytometry using protocols published by us previously.[17,18] Briefly, heparin-anticoagulated whole blood samples were obtained by venipuncture from healthy human volunteers with informed consent and as per guidelines

approved by the University of Kansas Human Subjects Experimentation Committee. Aliquots of whole human blood samples were stimulated with graded concentrations of either **8d** or **2** (used as a reference compound) in a 6-well polystyrene plate and incubated at 37°C in a rotary (100 rpm) incubator for 16.5 h. Negative (endotoxin free water) controls were included in each experiment. Following incubation, 200 μL aliquots of anticoagulated whole blood were stained with 20 μL of fluorochrome-conjugated antibodies at 37°C in the dark for 30 min. For triple color flow cytometry experiments, CD3-PE, CD56-APC, CD69-PE-Cy7 were used to analyze CD69 activation of each of the main peripheral blood lymphocyte populations: natural killer lymphocytes (NK cells: $CD3^{-}CD56^{+}$), cytokine-induced killer phenotype (CIK cells: $CD3^{+}CD56^{+}$), nominal B lymphocytes ($CD3^{-}CD56^{-}$), and nominal T lymphocytes ($CD3^{+}CD56^{-}$). Following staining, erythrocytes were lysed and leukocytes fixed in one step by mixing 200 μL of the samples in 4 mL pre-warmed Whole Blood Lyse/Fix Buffer (Becton-Dickinson Biosciences, San Jose, CA). After washing the cells twice at 200 g for 8 minutes in saline, the cells were transferred to a 96-well plate. Flow cytometry was performed using a BD FACSArray instrument in the tri-color mode (tri-color flow experiment) and two-color mode (two-color flow experiment) for acquisition on 100,000 gated events. Post-acquisition analyses were performed using FlowJo v 7.0 software (Treestar, Ashland, OR). Compensation for spillover was computed for each experiment on singly-stained samples.

Transcriptomal profiling in human PBMCs

Detailed procedures for transcriptomal profiling have been described by us previously.[17] Briefly, fresh human PBMC samples were stimulated with 10 μg/mL of **8d** and **2** for two hours, and total RNA was extracted from treated and negative control blood samples with QIAamp RNA Blood Mini Kit (Qiagen). Subsequently, 160 ng of each of the RNA samples was used. The Human Genome GeneChip U133 plus 2.0 oligonucleotide array (Affymetrix, Santa Clara, CA) was employed. Established standard protocols at the KU Genomics Facility were performed on cRNA target preparation, array hybridization, washing, staining and image scanning. The microarray data was first subjected to quality assessment using the Affymetrix GeneChip Operating Software (GCOS). QC criteria included low background, low noise, detection of positive controls, and a 5'/3' ratio of < 3.0. To facilitate direct comparison of gene expression data between different samples, the GeneChip data were first subjected to preprocessing. This step involved scaling (in GCOS) data from all chips to a target intensity value of 500, and further normalizations steps in GeneSpring GX (Agilent Technologies, Santa Clara, CA). Prior to identifying target genes, genes that were detected as non-expressed in all samples, i.e., those with absence calls, were filtered out. To identify genes whose expression was changed by our compounds, a fold change threshold of 2.0 between the compound treatment and the negative control was used.

Molecular modeling and induced fit docking

We used quantum mechanics/molecular mechanics (QM/MM) methods[61,62] for induced fit docking by calculating quantum mechanical charges for the ligand, while the macromolecule was handled using conventional molecular mechanics force fields. Correct bond orders were assigned, hydrogen atoms were added to the residues, and formal partial charges were assigned to atoms using OPLS-all atom force field.[63] The docking grid was generated using co-crystallized ligand as grid center. Ligands were modeled in Schrödinger molecular modeling software (Schrödinger, New York, NY) and were minimized to a gradient of $0.001 KCal/MolÅ^2$. The QM charges for ligands were obtained from Jaguar (Schrödinger), using the 3–21G basis set with the BLYP density functional theory.[64] Initial docking was performed with Glide[65,66] using 0.5 van der Waals (vdW) radius scaling factor for both ligand and protein. This soft docking procedure was applied to generate diverse docking solutions and top 20 poses for each ligand were retained. Finally, each ligand was

re-docked into its corresponding structures and the resulting complexes were ranked according to GlideScore.[65,66]

Supplementary Material

Refer to Web version on PubMed Central for supplementary material.

Acknowledgments

This work was supported by NIH/NIAID contract HSN272200900033C.

Abbreviations

APCs	antigen-presenting cells
CD69	cluster of differentiation 69
DCs	dendritic cells
EC_{50}	Half-maximal effective concentration
ESI-TOF	Electrospray ionization-time of flight
G-CSF	granulocyte colony-stimulating factor
GRO	growth-related oncogene
HEK	Human embryonic kidney
Ig	immunoglobulin
IFN	interferon
MPL	monophosphoryl lipid A
MIP	macrophage inflammatory protein
MHC	Major histocompatibility complex
NK	Natural killer
NF-κB	Nuclear factor-κB
NOD	nucleotide oligomerization domain
sAP	Secreted alkaline phosphatase
SAR	Structure activity relationship
TNF-α	Tumor necrosis factor-α
Th1	Helper T lymphocyte, type 1
Th2	Helper T lymphocyte, type 2
Tregs	T-regulatory cells
TGF	transforming growth factor
TLR	Toll like receptor

References

1. Hilleman MR. Vaccines in historic evolution and perspective: a narrative of vaccine discoveries. Vaccine. 2000; 18:1436–1447. [PubMed: 10618541]

2. Nabel GJ. Designing tomorrow's vaccines. N. Engl. J. Med. 2013; 368:551–560. [PubMed: 23388006]
3. Lessons from vaccine history. Nat. Med. 2012; 18:1717. [PubMed: 23223040]
4. Pashine A, Valiante NM, Ulmer JB. Targeting the innate immune response with improved vaccine adjuvants. Nat. Med. 2005; 11:S63–S68. [PubMed: 15812492]
5. Glenny AT, Pope CG, Waddington H, Wallace V. The antigenic value of toxoid precipitated by potassium-alum. J. Path. Bact. 1926; 29:38–45.
6. Garcon N, Van Mechelen M. Recent clinical experience with vaccines using MPL- and QS-21-containing adjuvant systems. Expert. Rev. Vaccines. 2011; 10:471–486. [PubMed: 21506645]
7. Relyveld EH, Bizzini B, Gupta RK. Rational approaches to reduce adverse reactions in man to vaccines containing tetanus and diphtheria toxoids. Vaccine. 1998; 16:1016–1023. [PubMed: 9682353]
8. Gupta RK. Aluminum compounds as vaccine adjuvants. Adv. Drug Deliv. Rev. 1998; 32:155–172. [PubMed: 10837642]
9. Loo YM, Gale M Jr. Immune signaling by RIG-I-like receptors. Immunity. 2011; 34:680–692. [PubMed: 21616437]
10. Kersse K, Bertrand MJ, Lamkanfi M, Vandenabeele P. NOD-like receptors and the innate immune system: coping with danger, damage and death. Cytokine Growth Factor Rev. 2011; 22:257–276. [PubMed: 21996492]
11. Clarke TB, Weiser JN. Intracellular sensors of extracellular bacteria. Immunol. Rev. 2011; 243:9–25. [PubMed: 21884164]
12. Kumagai Y, Takeuchi O, Akira S. Pathogen recognition by innate receptors. J. Infect. Chemother. 2008; 14:86–92. [PubMed: 18622669]
13. Akira S. Toll-like receptors and innate immunity. Adv. Immunol. 2001; 78:1–56. [PubMed: 11432202]
14. Akira S, Takeda K, Kaisho T. Toll-like receptors: critical proteins linking innate and acquired immunity. Nature Immunol. 2001; 2:675–680. [PubMed: 11477402]
15. Cottalorda A, Verschelde C, Marcais A, Tomkowiak M, Musette P, Uematsu S, Akira S, Marvel J, Bonnefoy-Berard N. TLR2 engagement on CD8 T cells lowers the threshold for optimal antigen-induced T cell activation. Eur. J. Immunol. 2006; 36:1684–1693. [PubMed: 16761317]
16. Kaisho T, Akira S. Toll-like receptors as adjuvant receptors. Biochim. Biophys. Acta. 2002; 1589:1–13. [PubMed: 11909637]
17. Hood JD, Warshakoon HJ, Kimbrell MR, Shukla NM, Malladi S, Wang X, David SA. Immunoprofiling toll-like receptor ligands: Comparison of immunostimulatory and proinflammatory profiles in ex vivo human blood models. Hum. Vaccin. 2010; 6:1–14.
18. Warshakoon HJ, Hood JD, Kimbrell MR, Malladi S, Wu WY, Shukla NM, Agnihotri G, Sil D, David SA. Potential adjuvantic properties of innate immune stimuli. Hum. Vaccin. 2009; 5:381–394. [PubMed: 19270494]
19. Agnihotri G, Crall BM, Lewis TC, Day TP, Balakrishna R, Warshakoon HJ, Malladi SS, David SA. Structure-activity relationships in toll-like receptor 2-agonists leading to simplified monoacyl lipopeptides. J. Med. Chem. 2011; 54:8148–8160. [PubMed: 22007676]
20. Salunke DB, Shukla NM, Yoo E, Crall BM, Balakrishna R, Malladi SS, David SA. Structure-Activity Relationships in Human Toll-like Receptor 2-Specific Monoacyl Lipopeptides. J. Med. Chem. 2012; 55:3353–3363. [PubMed: 22385476]
21. Wu W, Li R, Malladi SS, Warshakoon HJ, Kimbrell MR, Amolins MW, Ukani R, Datta A, David SA. Structure-activity relationships in toll-like receptor-2 agonistic diacylthioglycerol lipopeptides. J. Med. Chem. 2010; 53:3198–3213. [PubMed: 20302301]
22. Shukla NM, Kimbrell MR, Malladi SS, David SA. Regioisomerism-dependent TLR7 agonism and antagonism in an imidazoquinoline. Bioorg. Med. Chem. Lett. 2009; 19:2211–2214. [PubMed: 19285861]
23. Shukla NM, Malladi SS, Mutz CA, Balakrishna R, David SA. Structure-activity relationships in human toll-like receptor 7-active imidazoquinoline analogues. J. Med. Chem. 2010; 53:4450–4465. [PubMed: 20481492]

24. Shukla NM, Mutz CA, Ukani R, Warshakoon HJ, Moore DS, David SA. Syntheses of fluorescent imidazoquinoline conjugates as probes of Toll-like receptor 7. Bioorg. Med. Chem. Lett. 2010; 20:6384–6386. [PubMed: 20933417]
25. Shukla NM, Lewis TC, Day TP, Mutz CA, Ukani R, Hamilton CD, Balakrishna R, David SA. Toward self-adjuvanting subunit vaccines: model peptide and protein antigens incorporating covalently bound toll-like receptor-7 agonistic imidazoquinolines. Bioorg. Med. Chem. Lett. 2011; 21:3232–3236. [PubMed: 21549593]
26. Shukla NM, Mutz CA, Malladi SS, Warshakoon HJ, Balakrishna R, David SA. Toll-Like Receptor (TLR)-7 and −8 Modulatory Activities of Dimeric Imidazoquinolines. J. Med. Chem. 2012; 55:1106–1116. [PubMed: 22239408]
27. Kokatla HP, Yoo E, Salunke DB, Sil D, Ng CF, Balakrishna R, Malladi SS, Fox LM, David SA. Toll-like receptor-8 agonistic activities in C2, C4, and C8 modified thiazolo[4,5-*c*]quinolines. Org. Biomol. Chem. 2013; 11:1179–1198. [PubMed: 23314908]
28. Salunke DB, Yoo E, Shukla NM, Balakrishna R, Malladi SS, Serafin KJ, Day VW, Wang X, David SA. Structure-activity relationships in human Tolllike receptor 8-active 2,3-diamino-furo[2,3-*c*]pyridines. J. Med. Chem. 2012; 55:8137–8151. [PubMed: 22924757]
29. Agnihotri G, Ukani R, Malladi SS, Warshakoon HJ, Balakrishna R, Wang X, David SA. Structure-activity relationships in nucleotide oligomerization domain 1 (Nod1) agonistic gamma-glutamyldiaminopimelic acid derivatives. J. Med. Chem. 2011; 54:1490–1510. [PubMed: 21299227]
30. Ukani R, Lewis TC, Day TP, Wu W, Malladi SS, Warshakoon HJ, David SA. Potent adjuvantic activity of a CCR1-agonistic bis-quinoline. Bioorg. Med. Chem. Lett. 2012; 22:293–295. [PubMed: 22104149]
31. Gorden KB, Gorski KS, Gibson SJ, Kedl RM, Kieper WC, Qiu X, Tomai MA, Alkan SS, Vasilakos JP. Synthetic TLR agonists reveal functional differences between human TLR7 and TLR8. J. Immunol. 2005; 174:1259–1268. [PubMed: 15661881]
32. Philbin VJ, Levy O. Immunostimulatory activity of Toll-like receptor 8 agonists towards human leucocytes: basic mechanisms and translational opportunities. Biochem. Soc. Trans. 2007; 35:1485–1491. [PubMed: 18031250]
33. Qin J, Yao J, Cui G, Xiao H, Kim TW, Fraczek J, Wightman P, Sato S, Akira S, Puel A, Casanova JL, Su B, Li X. TLR8-mediated NF-kappaB and JNK activation are TAK1-independent and MEKK3-dependent. J. Biol. Chem. 2006; 281:21013–21021. [PubMed: 16737960]
34. Levy O, Suter EE, Miller RL, Wessels MR. Unique efficacy of Toll-like receptor 8 agonists in activating human neonatal antigen-presenting cells. Blood. 2006; 108:1284–1290. [PubMed: 16638933]
35. Smith TR, Kumar V. Revival of CD8+ Treg-mediated suppression. Trends Immunol. 2008; 29:337–342. [PubMed: 18514574]
36. Gupta S, Shang W, Sun Z. Mechanisms regulating the development and function of natural regulatory T cells. Arch. Immunol. Ther. Exp. (Warsz.). 2008; 56:85–102. [PubMed: 18373240]
37. Cools N, Ponsaerts P, Van Tendeloo VF, Berneman ZN. Regulatory T cells and human disease. Clin. Dev. Immunol. 2007; 2007:89195. [PubMed: 18317534]
38. Germain RN. Special regulatory T-cell review: A rose by any other name: from suppressor T cells to Tregs, approbation to unbridled enthusiasm. Immunology. 2008; 123:20–27. [PubMed: 18154615]
39. Wan YY, Flavell RA. Regulatory T cells, transforming growth factor-beta, and immune suppression. Proc. Am. Thorac. Soc. 2007; 4:271–276. [PubMed: 17607012]
40. Kim CH. Trafficking of FoxP3+ regulatory T cells: myths and facts. Arch. Immunol. Ther. Exp. (Warsz.). 2007; 55:151–159. [PubMed: 17557143]
41. Long ET, Wood KJ. Regulatory T cells--a journey from rodents to the clinic. Front Biosci. 2007; 12:4042–4049. [PubMed: 17485357]
42. Sutmuller RP, Morgan ME, Netea MG, Grauer O, Adema GJ. Toll-like receptors on regulatory T cells: expanding immune regulation. Trends Immunol. 2006; 27:387–393. [PubMed: 16814607]

43. Jurk M, Heil F, Vollmer J, Schetter C, Krieg AM, Wagner H, Lipford G, Bauer S. Human TLR7 or TLR8 independently confer responsiveness to the antiviral compound R-848. Nat. Immunol. 2002; 3:499. [PubMed: 12032557]
44. Gerster JF, Lindstrom KJ, Marszalek GJ, Merrill BA, Mickelson JW, Rice MJ. Oxazolo, thiazolo and selenazolo [4,5-*c*]-quinolin-4-amines and analogs thereof. [WO 00/06577]. 2000:1–102.
45. Gerster JF, Lindstrom KJ, Miller RL, Tomai MA, Birmachu W, Bomersine SN, Gibson SJ, Imbertson LM, Jacobson JR, Knafla RT, Maye PV, Nikolaides N, Oneyemi FY, Parkhurst GJ, Pecore SE, Reiter MJ, Scribner LS, Testerman TL, Thompson NJ, Wagner TL, Weeks CE, Andre JD, Lagain D, Bastard Y, Lupu M. Synthesis and structure-activity-relationships of 1H-imidazo[4,5-*c*]quinolines that induce interferon production. J. Med. Chem. 2005; 48:3481–3491. [PubMed: 15887957]
46. Prince RB, Merrill BA, Heppner PD, Kshirsagar TA, Wurst JR, Manske KJ, Rice MJ. Alkyloxy substituted thiazoloquinolines and thiolonaphthyridines. [WO 2006/086449]. 2006:1–193.
47. Prince RB, Rice MJ, Wurst JR, Merrill BA, Kshirsagar TA, Heppner PD. Aryloxy and arylalkyleneoxy substituted thiazoloquinolines and thiazolonapthyridines. [WO 2006/009826 A1]. 2006:1–104.
48. Lu H, Dietsch GN, Matthews MA, Yang Y, Ghanekar S, Inokuma M, Suni M, Maino VC, Henderson KE, Howbert JJ, Disis ML, Hershberg RM. VTX-2337 is a novel TLR8 agonist that activates NK cells and augments ADCC. Clin. Cancer Res. 2012; 18:499–509. [PubMed: 22128302]
49. Dowling DJ, Tan Z, Prokopowicz ZM, Palmer CD, Matthews MA, Dietsch GN, Hershberg RM, Levy O. The Ultra-Potent and Selective TLR8 Agonist VTX-294 Activates Human Newborn and Adult Leukocytes. PLoS. ONE. 2013; 8:e58164. [PubMed: 23483986]
50. Venkataraman S, Barange DK, Pal M. One-pot synthesis of 2-substituted furo[3,2-*c*]quinolines via tandem coupling–cyclization under Pd/C-copper catalysis. Tetrahedron Lett. 2006:7317–7322.
51. Gaddam B, Polsetti DR, Guzel M, Victory S, Kostura M. Substituted pyridine derivatives, pharmaceutical compositions, and methods of use to treat oxidative stress. 61/234,498[WO 2011/022216]. 2011:1–47.
52. Shukla NM, Salunke DB, Balakrishna R, Mutz CA, Malladi SS, David SA. Potent adjuvanticity of a pure TLR7-agonistic imidazoquinoline dendrimer. PLoS. ONE. 2012; 7:e43612. [PubMed: 22952720]
53. Miller KA, Suresh Kumar EVK, Wood SJ, Cromer JR, Datta A, David SA. Lipopolysaccharide Sequestrants: Structural Correlates of Activity and Toxicity in Novel Acylhomospermines. J. Med. Chem. 2005; 48:2589–2599. [PubMed: 15801849]
54. Sil D, Shrestha A, Kimbrell MR, Nguyen TB, Adisechan AK, Balakrishna R, Abbo BG, Malladi S, Miller KA, Short S, Cromer JR, Arora S, Datta A, David SA. Bound to Shock: Protection from Lethal Endotoxemic Shock by a Novel, Nontoxic, Alkylpolyamine Lipopolysaccharide Sequestrant. Antimicrob. Agents Chemother. 2007; 51:2811–2819. [PubMed: 17548488]
55. Shukla NM, Malladi SS, Day V, David SA. Preliminary evaluation of a 3H imidazoquinoline library as dual TLR7/TLR8 antagonists. Bioorg. Med. Chem. 2011; 19:3801–3811. [PubMed: 21620714]
56. Tanji H, Ohto U, Shibata T, Miyake K, Shimizu T. Structural reorganization of the Toll-like receptor 8 dimer induced by agonistic ligands. Science. 2013; 339:1426–1429. [PubMed: 23520111]
57. Spyrakis F, BidonChanal A, Barril X, Luque FJ. Protein flexibility and ligand recognition: challenges for molecular modeling. Curr. Top. Med. Chem. 2011; 11:192–210. [PubMed: 20939788]
58. Wlodarski T, Zagrovic B. Conformational selection and induced fit mechanism underlie specificity in noncovalent interactions with ubiquitin. Proc. Natl. Acad. Sci. U. S. A. 2009; 106:19346–19351. [PubMed: 19887638]
59. David SA, Smith MS, Lopez G, Mukherjee S, Buch S, Narayan O. Selective transmission of R5-tropic HIV-1 from dendritic cells to resting $CD4^+$ T cells. AIDS Res. Human Retrovir. 2001; 17:59–68. [PubMed: 11177384]

60. Kimbrell MR, Warshakoon H, Cromer JR, Malladi S, Hood JD, Balakrishna R, Scholdberg TA, David SA. Comparison of the immunostimulatory and proinflammatory activities of candidate Gram-positive endotoxins, lipoteichoic acid, peptidoglycan, and lipopeptides, in murine and human cells. Immunol. Lett. 2008; 118:132–141. [PubMed: 18468694]

61. Alves CN, Marti S, Castillo R, Andres J, Moliner V, Tunon I. and Silla, E. A quantum mechanics/molecular mechanics study of the protein-ligand interaction for inhibitors of HIV-1 integrase. Chemistry. 2007; 13:7715–7724. [PubMed: 17570717]

62. Murphy RB, Philipp DM, Friesner RA. A mixed quantum mechanics/molecular mechanics (QM/MM) method for large-scale modeling of chemistry in protein environments. J. Comput. Chem. 2000; 21:1442–1457.

63. Jorgensen WL, Schyman P. Treatment of Halogen Bonding in the OPLS-AA Force Field; Application to Potent Anti-HIV Agents. J. Chem. Theory. Comput. 2012; 8:3895–3801. [PubMed: 23329896]

64. Antony J, Grimme S. Density functional theory including dispersion corrections for intermolecular interactions in a large benchmark set of biologically relevant molecules. Phys. Chem. Chem. Phys. 2006; 8:5287–5293. [PubMed: 19810407]

65. Repasky MP, Shelley M, Friesner RA. Flexible ligand docking with Glide. Curr. Protoc. Bioinformatics. 2007; Chapter 8 Unit.

66. Halgren TA, Murphy RB, Friesner RA, Beard HS, Frye LL, Pollard WT, Banks JL. Glide: a new approach for rapid, accurate docking and scoring. 2. Enrichment factors in database screening. J. Med. Chem. 2004; 47:1750–1759. [PubMed: 15027866]

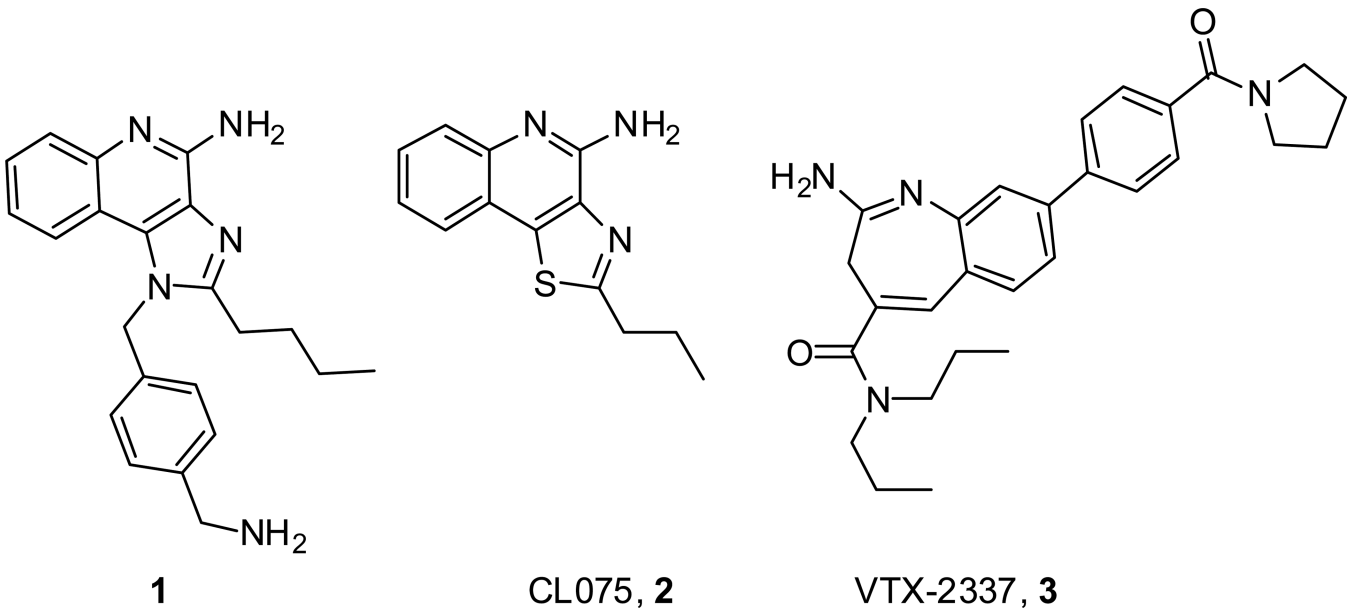

Figure 1.
Representative TLR8/7 dual-agonistic heterocyclic small molecules.

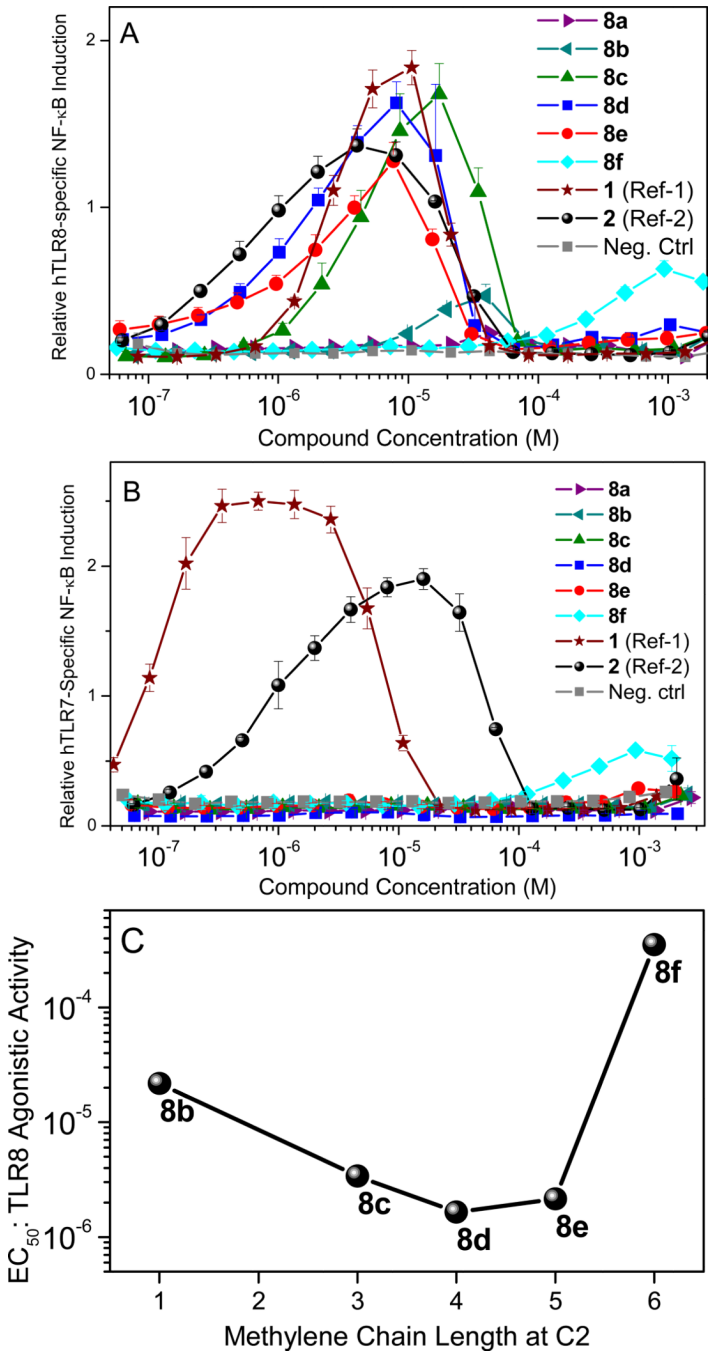

Figure 2.

Dose-response profiles of human TLR8 (Panel A) and human TLR7 (Panel B) agonism by select C2-alkyl furo[2,3-*c*]quinolines. Error bars represent standard deviations obtained on quadruplicates. Dual TLR7/8-agonistic compounds **1** and **2** were used as comparators. C. Potency of TLR8 agonism (EC50 values) of a homologous series of C2-alkyl analogues. Compound **8a** was inactive.

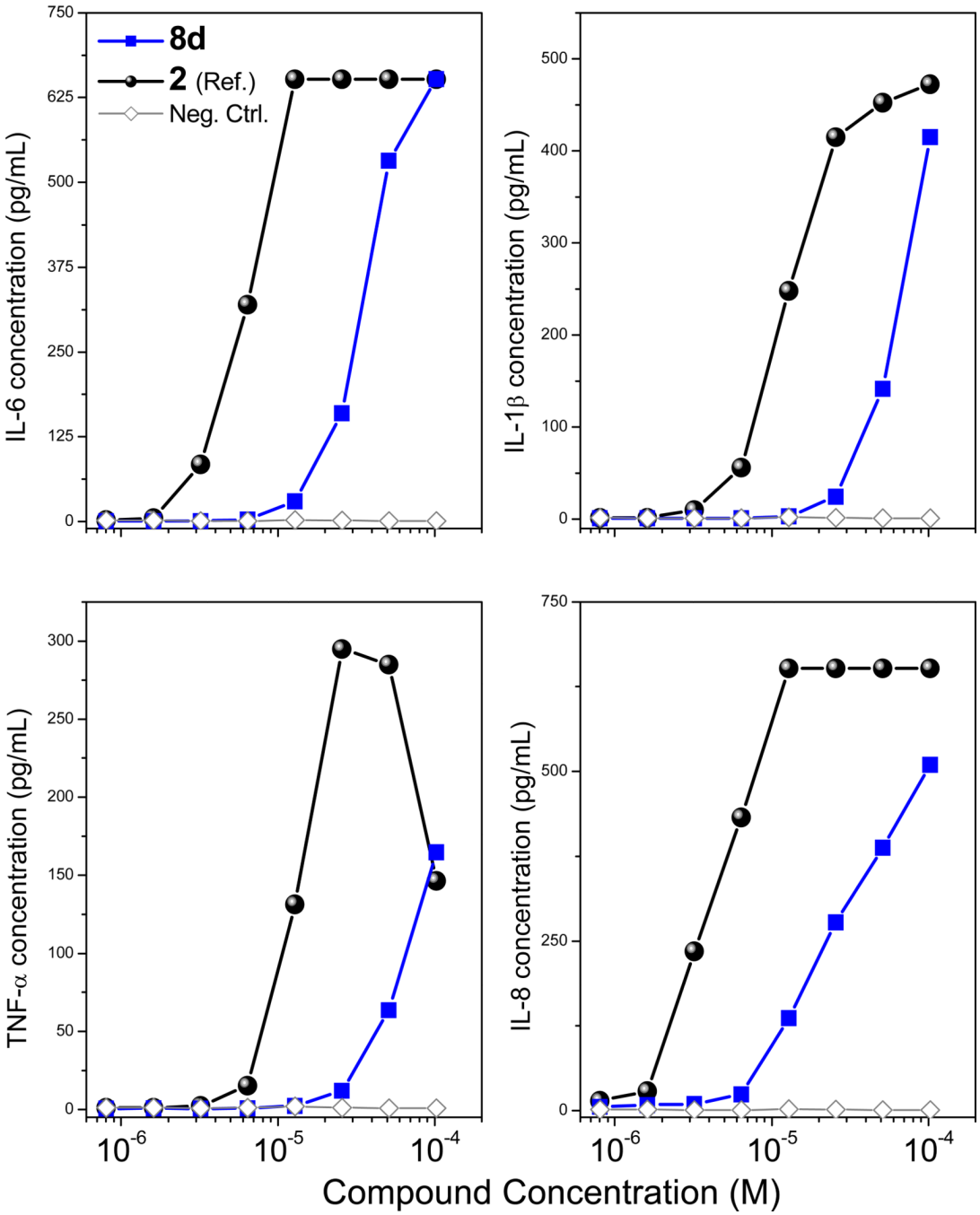

Figure 3.
Proinflammatory cytokine induction profiles of **8d** in human blood. **2** was used as reference/ comparator compound. Means of duplicate values of a representative experiment is shown.

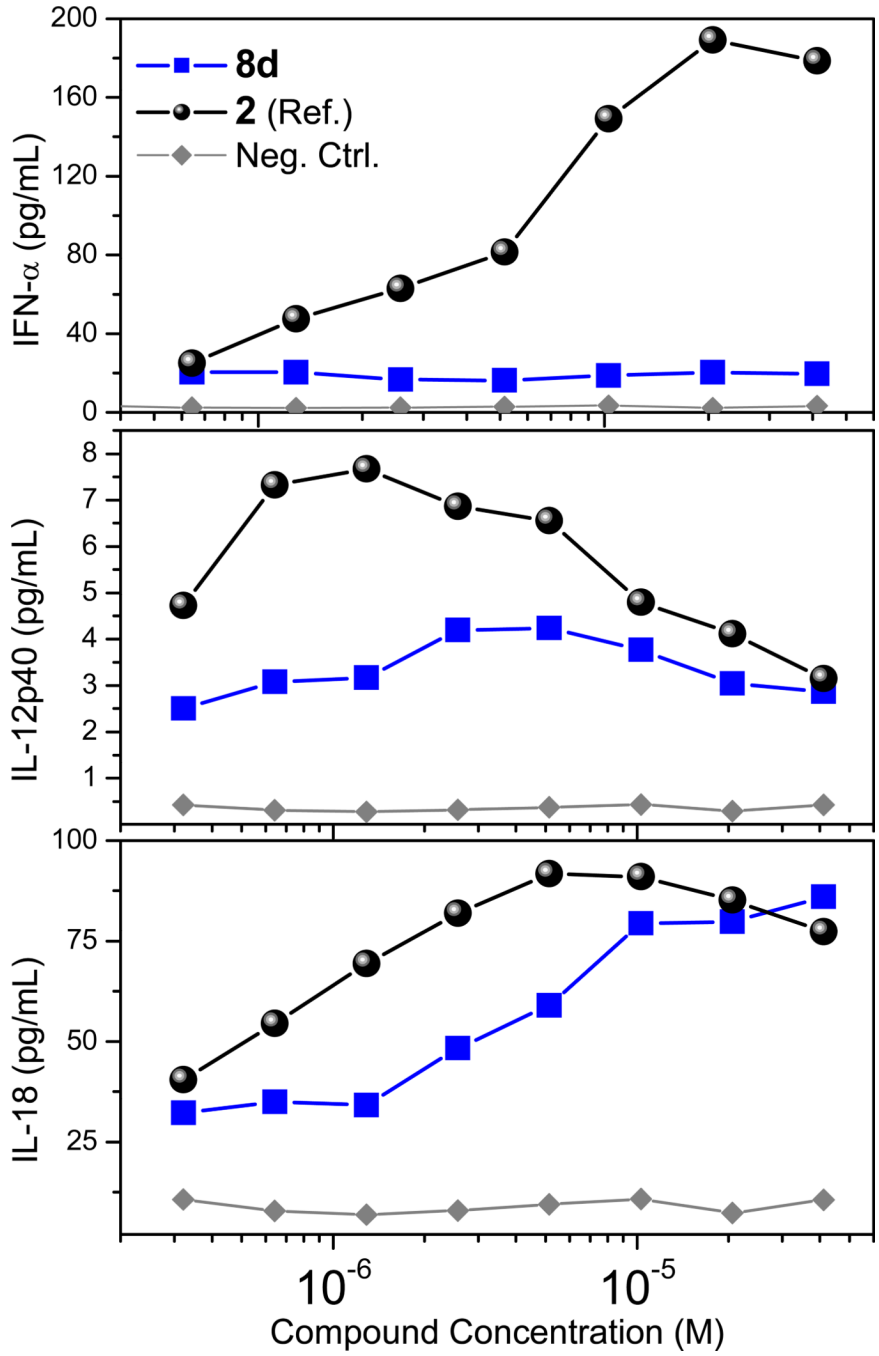

Figure 4.

Dose-response profiles of IL-12p40 and IL-18 induction and the absence of IFN-α by **8d. 2** was used as reference/comparator compound. Means of duplicate values of a representative experiment is shown.

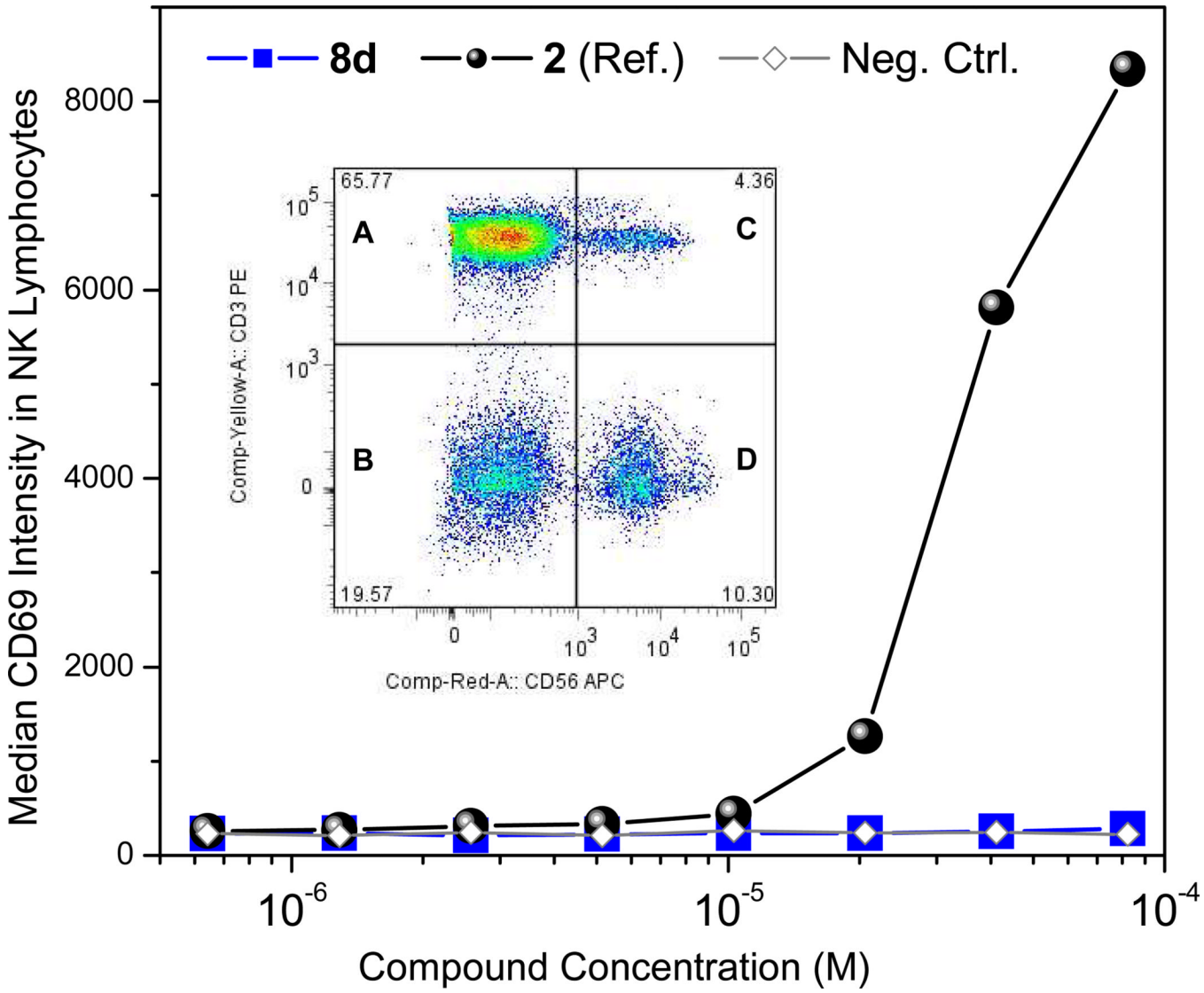

Figure 5.

Absence of CD69 upregulation in human natural killer cells by **8d**. Inset: gating on lymphocytes showing $CD3^{+}CD56^{-}$ (T cells, Quadrant A), $CD3^{-}CD56^{-}$ (nominal B cells, Quadrant B), $CD3^{-}CD56^{+}$ (cytokine-induced killer cells, Quadrant C), and $CD3^{-}CD56^{+}$ (natural killer cells, Quadrant D).

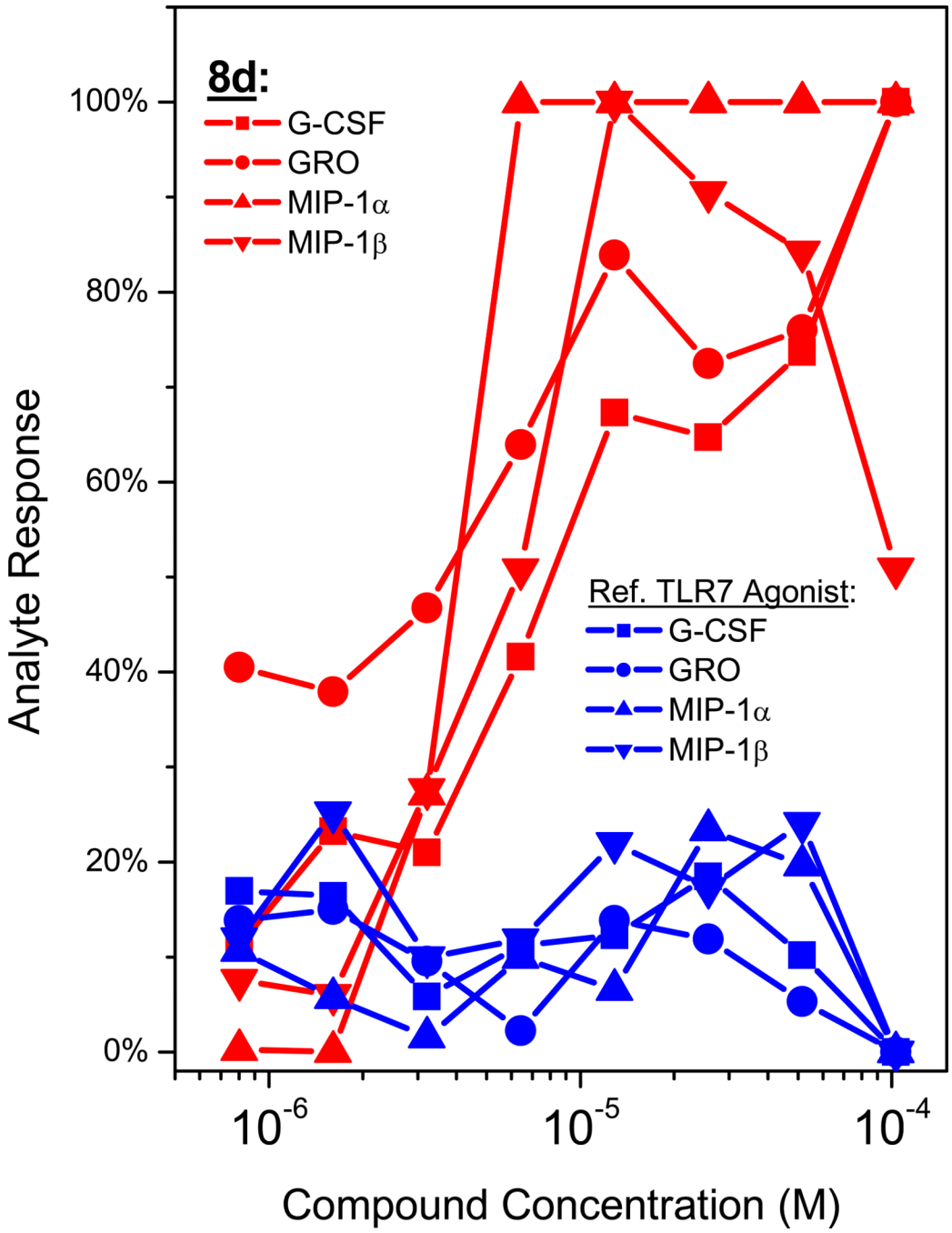

Figure 6.

Disparate responses in select analytes (out of 41 analytes) in human PBMCs. G-CSF, GRO, MIP-1α, and MIP-1β are induced by **8d** (and **2**, data not shown), but not by a pure TLR7 agonistic imidazoquinoline. Dose responses represent percent maximal response (G-CSF: 622 pg/mL, GRO: 515 pg/mL, MIP-1α: 10780 pg/mL, and MIP-1β: 10374 pg/mL). Means of duplicate values of a representative experiment is shown. Analytes were below detection limits for negative controls (medium alone), and are not shown for clarity.

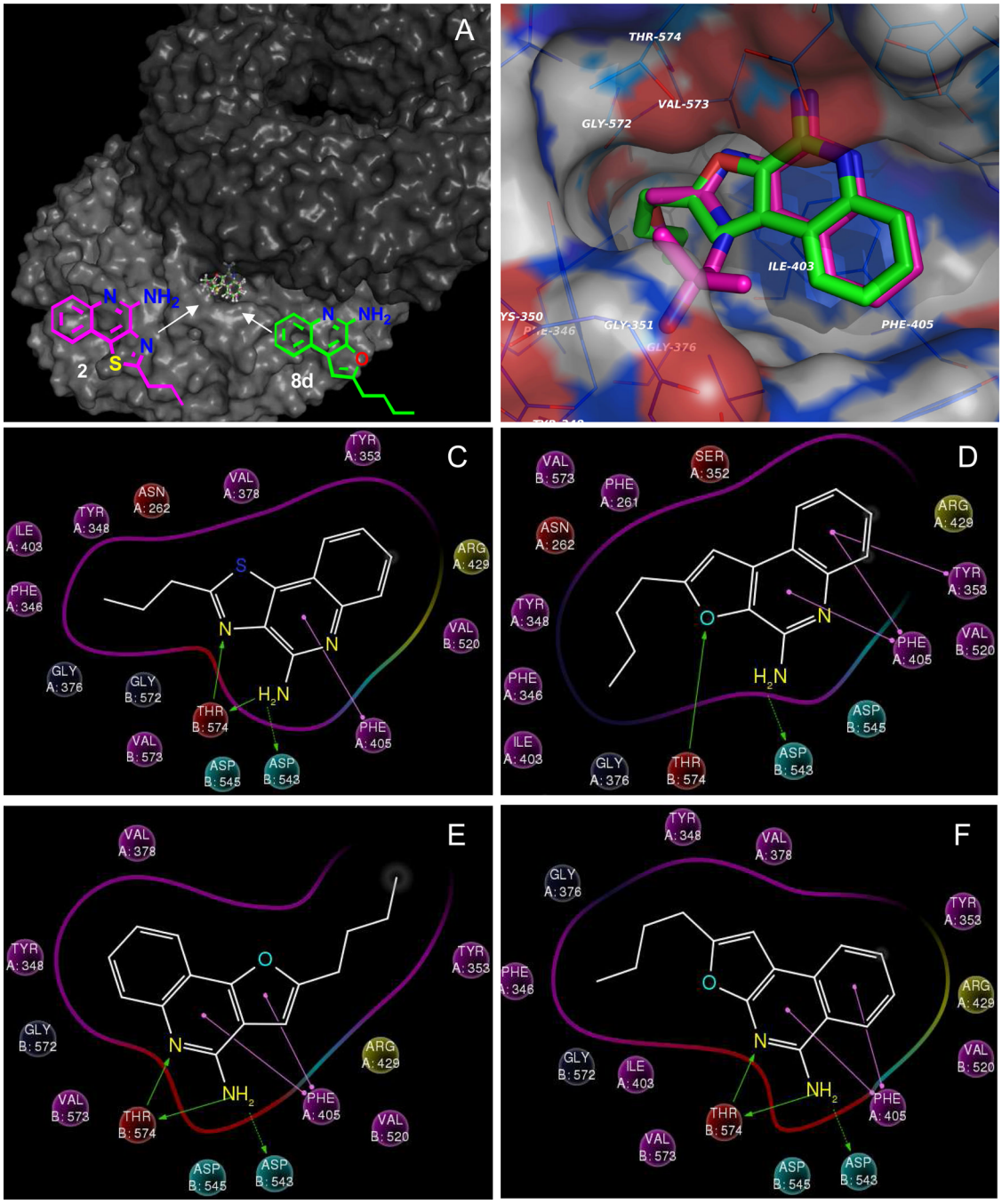

Figure 7.

Induced fit docking of ligands in human TLR8 (PDB ID: 3W3K). A. Both **2** and **8d** occupy the same binding pocket. B. The binding modes of the TLR7/8-dual active imidazoquinoline CL097 and **8d** are superimposable. C–F. Binding site interactions of **2, 8d, 13b**, and **18**, respectively.

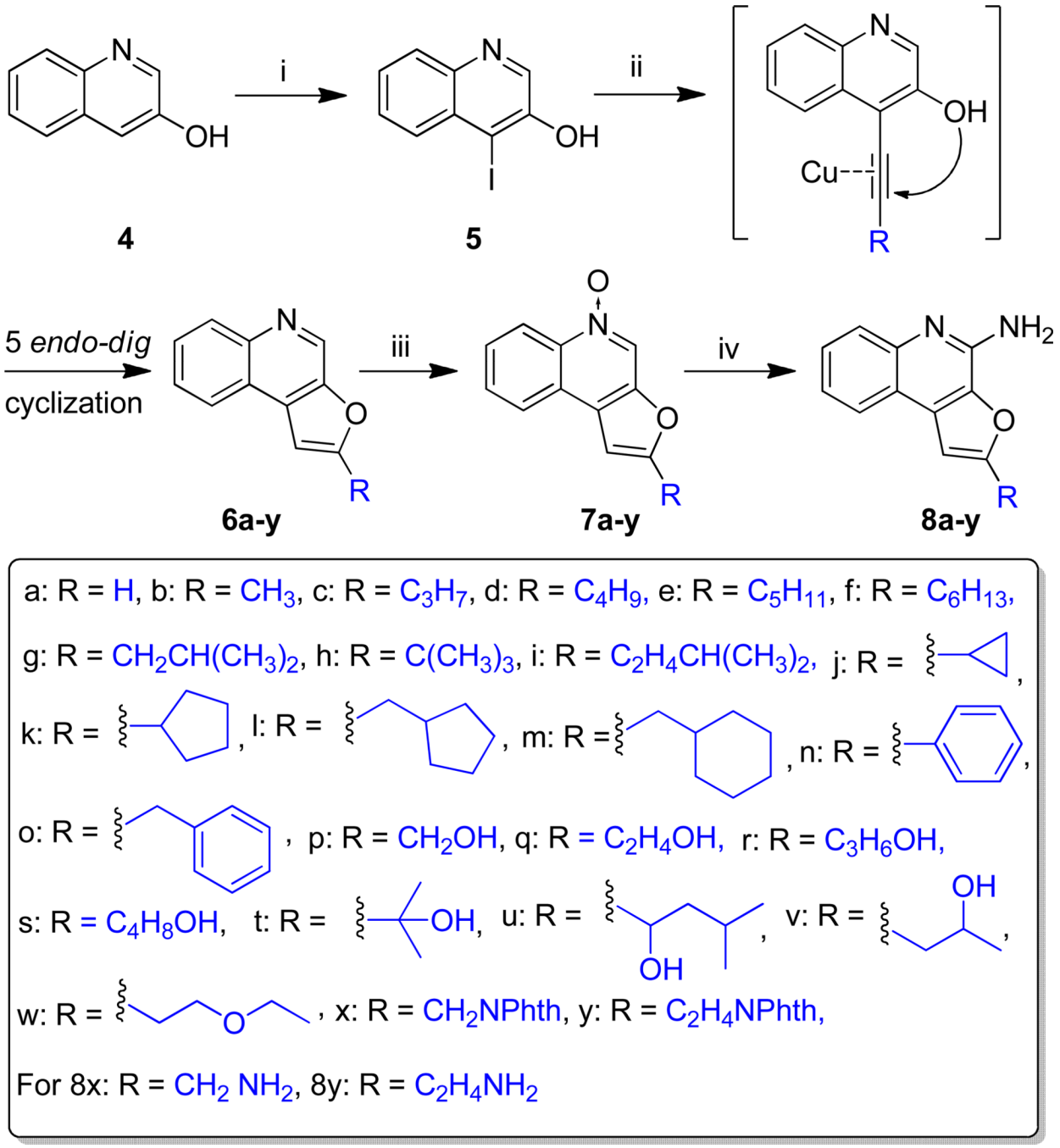

Scheme 1.

Syntheses of C2-alkylfuro[2,3-*c*]quinoline analogues. Reagents: (i) I_2, KI, NaOH; (ii) $Pd(PPh_3)_4$, CuI alkyne, Et_3N:CH_3CN (1:3); (iii) *m*-CPBA, $CHCl_3$; (iv) (a) benzoyl isocyanate, CH_2Cl_2, (b) $NaOCH_3$, MeOH.

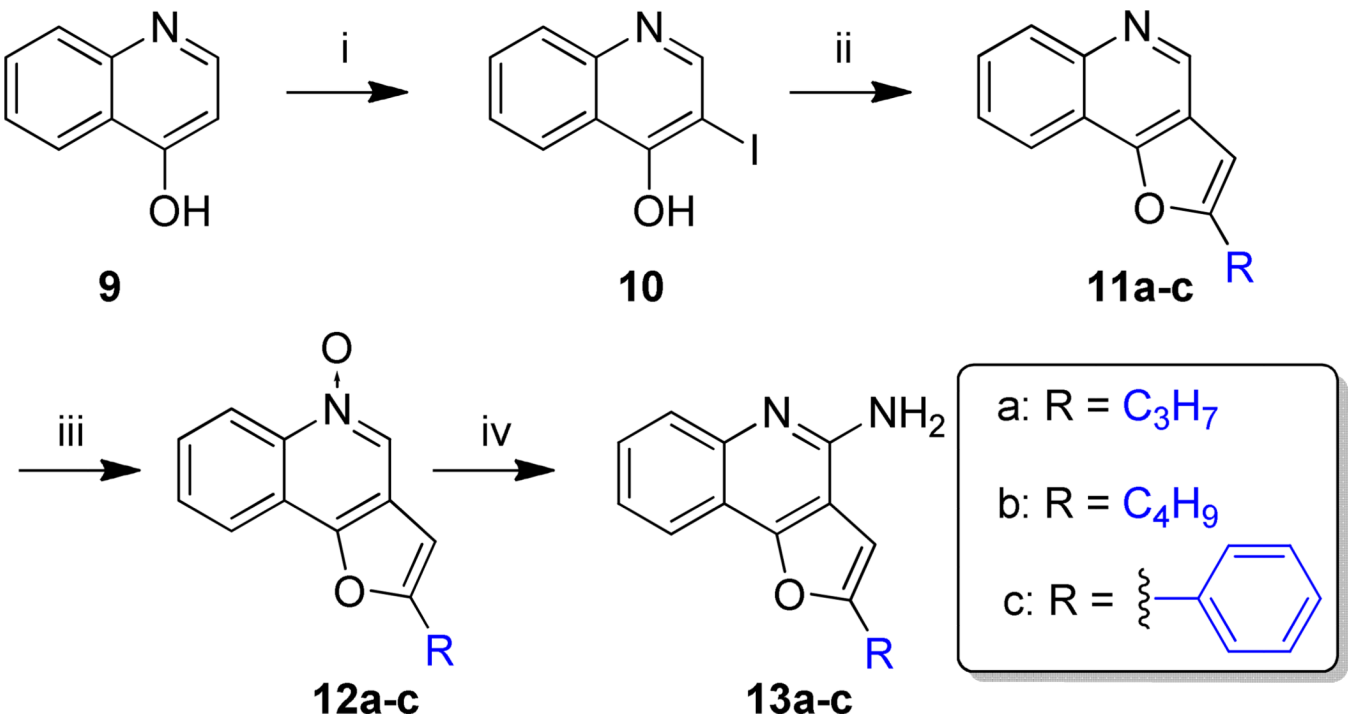

Scheme 2.

Syntheses of C2-alkylfuro[3,2-*c*]quinoline analogues. Reagents: (i) I_2, KI, NaOH; (ii) Pd(PPh3)4 CuI alkyne, Et3N:CH3CN (1:3); (iii) *m*-CPBA, $CHCl_3$; (iv) (a) benzoyl isocyanate, CH_2Cl_2, (b) $NaOCH_3$, MeOH.

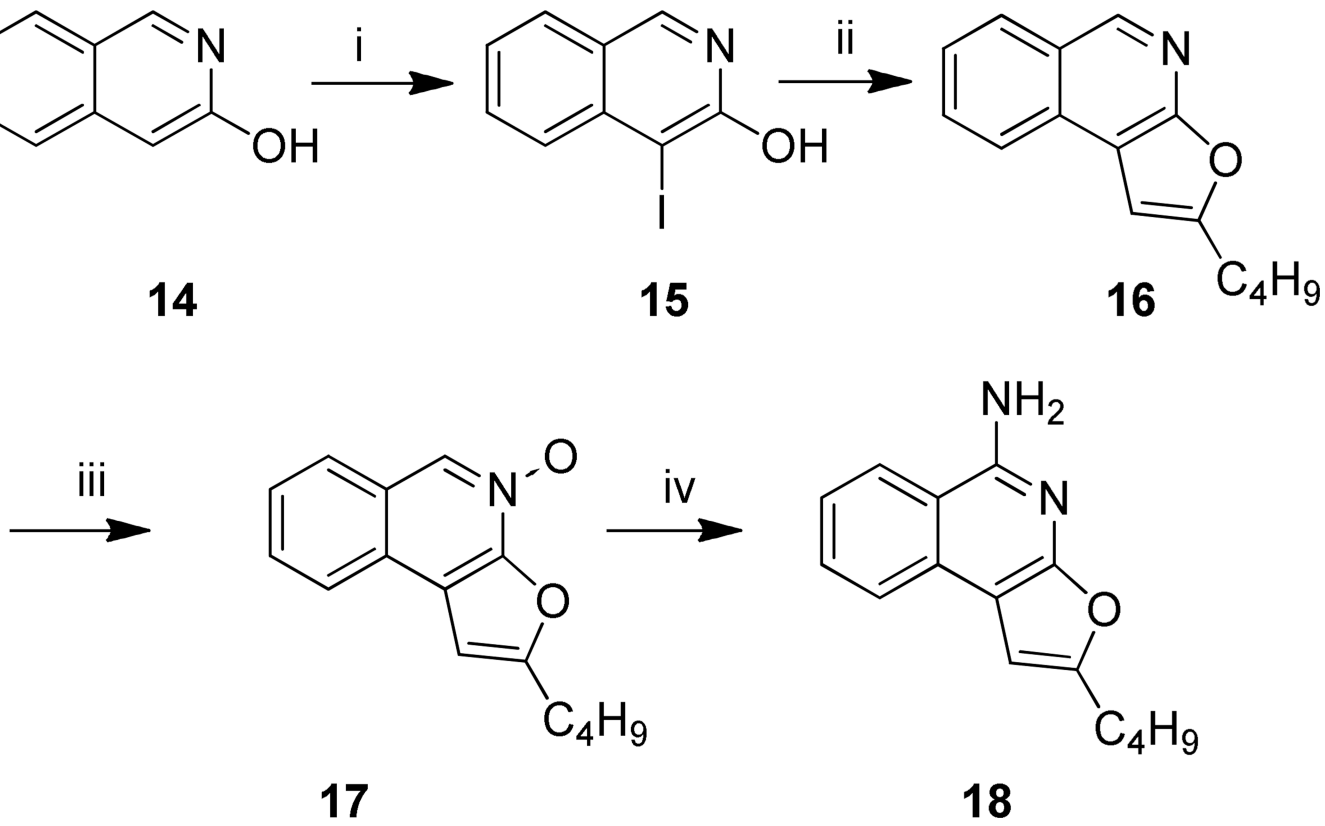

Scheme 3.

Syntheses of C2-alkylfuro[2,3-*c*]isoquinoline analogues. Reagents: (i) I_2, KI, NaOH; (ii) $Pd(PPh_3)_4$, CuI alkyne, Et_3N:CH_3CN (1:3); (iii) *m*-CPBA, $CHCl_3$; (iv) (a) benzoyl isocyanate, CH_2Cl_2, (b) $NaOCH_3$, MeOH.

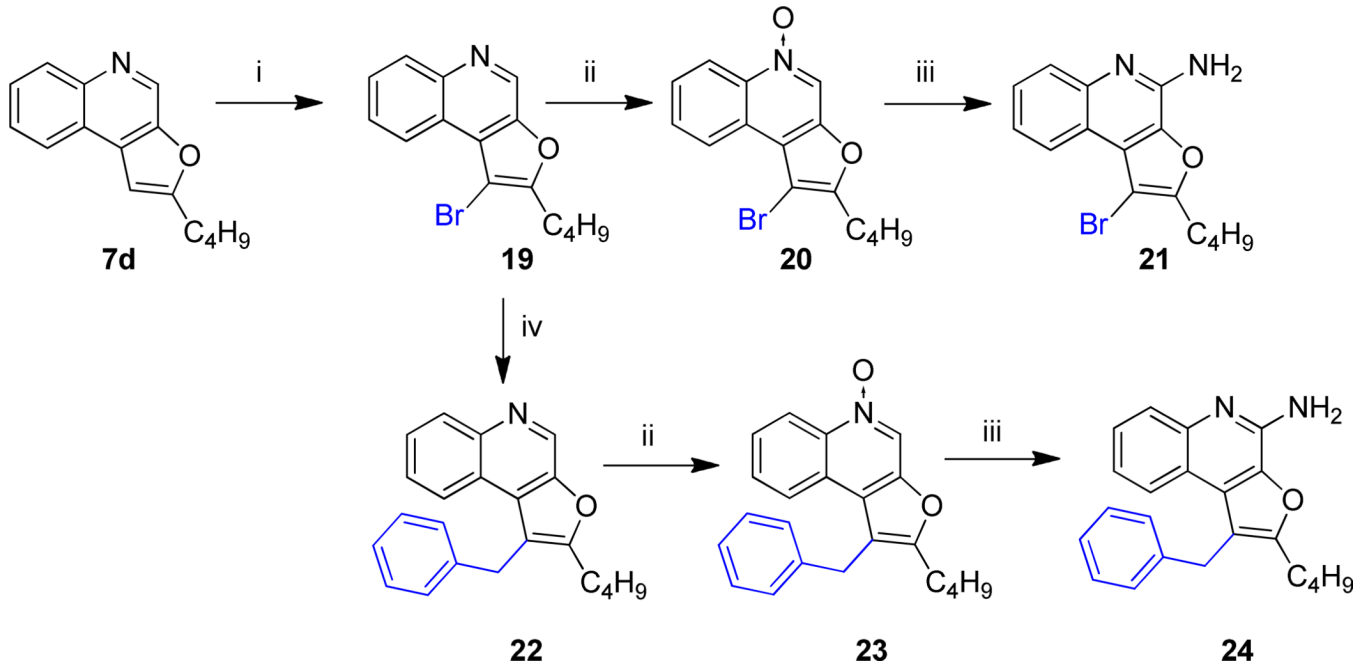

Scheme 4.

Syntheses of C1- substituted furo[2,3-*c*]quinoline analogues. Reagents: (i) Br_2, CH_2Cl_2; (ii) *m*-CPBA $CHCl_3$; (iii) (a) benzoyl isocyanate, CH_2Cl_2, (b) $NaOCH_3$, MeOH; (iv) $Pd(dppf)Cl_2$, 2-benzyl-4,4,5,5-tetramethyl-1,3,2-dioxaborolane, Cs_2CO_3 1,4-Dioxane

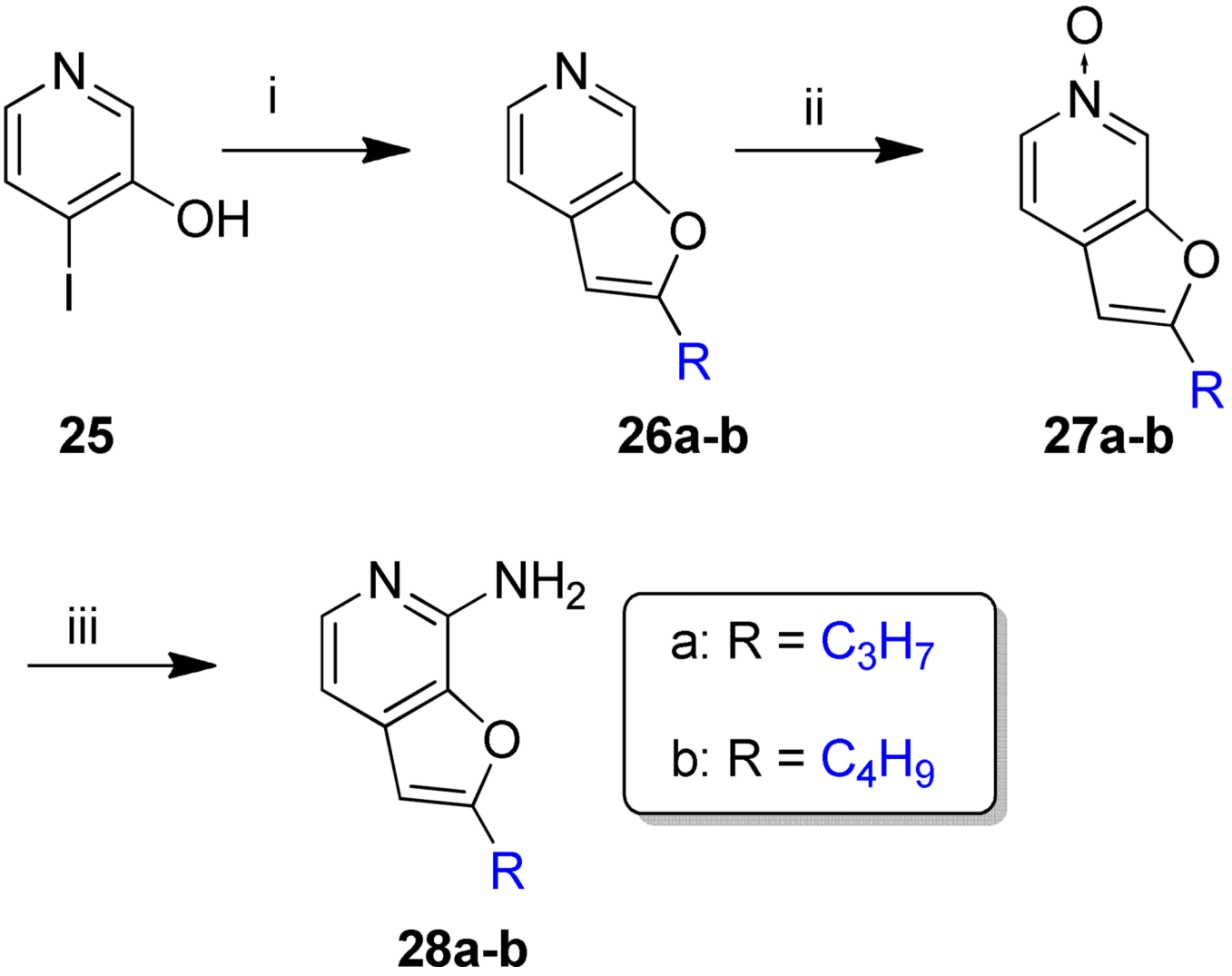

Scheme 5.

Syntheses of C2-alkylfuro[2,3-*c*]pyridine analogues. Reagents: (i) $Pd(PPh_3)_4$, CuI alkyne, Et_3N:CH_3CN (1:3); (ii) *m*-CPBA, $CHCl_3$; (iii) (a) benzoyl isocyanate, CH_2Cl_2, (b) $NaOCH_3$, MeOH.

Table 1

Transcriptomal profiling of **8d** in human PBMCs

Probeset ID	Gene Symbol	Gene Title	Log(FC) 2 vs Neg.Ctrl	Log(FC) 8d vs Neg.Ctrl
208375_at	IFNA1	interferon, alpha 1	7.38297	0.5418
	IFNA1 ///			
208344_x_at	IFNA13	interferon, alpha 1///13	5.36195	0.85859
208261_x_at	IFNA10	interferon, alpha 10	5.87577	0.7771
211405_x_at	IFNA17	interferon, alpha 17	4.25712	0.81187
211145_x_at	IFNA21	interferon, alpha 21	4.96822	0.58271
214569_at	IFNA5	interferon, alpha 5	7.03922	1.22985
208259_x_at	IFNA7	interferon, alpha 7	5.77059	0.80266
207932_at	IFNA8	interferon, alpha 8	4.18566	0.61895
210354_at	IFNG	interferon, gamma	5.60123	4.54852
204470_at	CXCL1	chemokine (C-X-C motif) ligand 1	0.88813	1.99629
209774_x_at	CXCL2	chemokine (C-X-C motif) ligand 2	2.83012	2.8543
207850_at	CXCL3	chemokine (C-X-C motif) ligand 3	1.47026	1.75638
215101_s_at	CXCL5	chemokine (C-X-C motif) ligand 5	1.51721	2.39582
203915_at	CXCL9	chemokine (C-X-C motif) ligand 9	1.88404	0.81365
204533_at	CXCL10	chemokine (C-X-C motif) ligand 10	7.689	6.42653
210163_at	CXCL11	chemokine (C-X-C motif) ligand 11	8.89003	6.50285
211122_s_at	CXCL11	chemokine (C-X-C motif) ligand 11	9.00636	6.56354
210118_s_at	IL1A	interleukin 1, alpha	4.67389	4.82369
205067_at	IL1B	interleukin 1, beta	2.45708	2.44858
216243_s_at	IL1RN	interleukin 1 receptor antagonist	3.97769	3.66761
207538_at	IL4	interleukin 4	2.20255	2.24232
205207_at	IL6	interleukin 6	7.85102	7.67767
		interleukin 12B (natural killer cell		
207901_at	IL12B	stimulatory factor 2)	5.84181	3.26706
207844_at	IL13	interleukin 13	1.57695	2.04086
205992_s_at	IL15	interleukin 15	1.16516	1.06962
209827_s_at	IL16	interleukin 16	-1.7103	-0.64723
206295_at	IL18	interleukin 18	2.64035	2.40756
207072_at	IL18RAP	interleukin 18 receptor accessory protein	1.12674	0.51353
224071_at	IL20	interleukin 20	0.31683	0.81046
222974_at	IL22	interleukin 22	2.16422	0.38534
220054_at	IL23A	interleukin 23, alpha subunit p19	4.73191	4.96526
206569_at	IL24	interleukin 24	-0.6150	-0.00233
205926_at	IL27RA	interleukin 27 receptor, alpha	0.20872	0.16269
1552915_at	IL28A	interleukin 28A (interferon, lambda 2)	1.65564	0.59624
		interleukin 28 receptor, alpha (interferon,		
244261_at	IL28RA	Lambda receptor)	1.13284	0.78929

Probeset ID	Gene Symbol	Gene Title	Log(FC) 2 vs Neg.Ctrl	Log(FC) 8d vs Neg.Ctrl
1552917_at	IL29	interleukin 29 (interferon, lambda 1)	1.02924	0.76252
203828_s_at	IL32	interleukin 32	0.35684	0.70521
207113_s_at	TNF	tumor necrosis factor	3.81754	3.3126
206025_s_at	TNFAIP6	tumor necrosis factor, alpha-induced Protein 6	4.28297	4.17629